MOLECULAR AND CELLULAR BIOLOGY, Sept. 1997, p. 5437–5452 Vol. 17, No. 9
0270-7306/97/$04.00+0

Clusters of S1 Nuclease-Hypersensitive Sites Induced In Vivo by DNA Damage

JEAN LEGAULT, ALAIN TREMBLAY, DINDIAL RAMOTAR,† AND MARC-EDOUARD MIRAULT*

Unité de Santé et Environnement, Pavillon CHUL, Centre de Recherche du CHUQ et Université Laval, Sainte-Foy, Québec, Canada G1V 4G2

Received 7 March 1997/Returned for modification 8 April 1997/Accepted 6 June 1997

DNA end-labeling procedures were used to analyze both the frequency and distribution of DNA strand breaks in mammalian cells exposed or not to different types of DNA-damaging agents. The 3′ ends were labeled by T4 DNA polymerase-catalyzed nucleotide exchange carried out in the absence or presence of *Escherichia coli* endonuclease IV to cleave abasic sites and remove 3′ blocking groups. Using this sensitive assay, we show that DNA isolated from human cells or mouse tissues contains variable basal levels of DNA strand interruptions which are associated with normal bioprocesses, including DNA replication and repair. On the other hand, distinct dose-dependent patterns of DNA damage were assessed quantitatively in cultured human cells exposed briefly to menadione, methylmethane sulfonate, topoisomerase II inhibitors, or gamma rays. In vivo induction of single-strand breaks and abasic sites by methylmethane sulfonate was also measured in several mouse tissues. The genomic distribution of these lesions was investigated by DNA cleavage with the single-strand-specific S1 nuclease. Strikingly similar cleavage patterns were obtained with all DNA-damaging agents tested, indicating that the majority of S1-hypersensitive sites detected were not randomly distributed over the genome but apparently were clustered in damage-sensitive regions. The parallel disappearance of 3′ ends and loss of S1-hypersensitive sites during post-gamma-irradiation repair periods indicates that these sites were rapidly repaired single-strand breaks or gaps (2- to 3-min half-life). Comparison of S1 cleavage patterns obtained with gamma-irradiated DNA and gamma-irradiated cells shows that chromatin structure was the primary determinant of the distribution of the DNA damage detected.

DNA is intrinsically unstable: it undergoes spontaneous hydrolysis of labile *N*-glycosyl bonds, as well as oxidation and nonenzymatic methylation at significant rates in vivo (47). These processes are thought to contribute to mutagenesis, carcinogenesis, and aging (2, 3) and are suspected to be amplified by a plethora of environmental pollutants. Reactive oxygen species (ROS) such as superoxide radicals (O_2^-) and H_2O_2 are generated in all aerobic cells (19). Excess production of these ROS by endogenous sources, for example, mitochondria and activated leukocytes, or by exogenous sources such as redox-cycling quinones (75) will exacerbate oxidative damage to cellular DNA (33, 54). The toxicity of these ROS is thought to result at least in part from their conversion to the highly reactive hydroxyl radical by transition metal-catalyzed Fenton-type reactions (4, 25). This radical is also formed by the interaction of ionizing radiation with water, e.g., within cells (78), and is known to induce a broad spectrum of DNA lesions, including base and sugar modifications, base loss, and DNA strand breaks (8, 9). The most frequent lesions detected in cells exposed to ionizing radiation are oxidized apurinic/apyrimidinic (AP) (abasic) sites (27) and single-strand breaks, most of which are terminated with blocked 3′ ends in DNA irradiated in vitro (9). AP sites are thought to be one of the most commonly produced DNA lesions (47), which may result from any condition that leads to base modification (e.g., alkylation) and involves base excision repair initiated by *N*-glycosylases (20). It is thus not surprising that all organisms possess AP endonucleases that hydrolyze abasic sites (13, 62, 79), thereby producing transient DNA strand breaks. Some AP endonucleases, for example, *Escherichia coli* endonuclease IV (46), also possess a 3′-diesterase activity that can remove the blocked 3′ ends of DNA strand breaks resulting from oxidative damage. Both cellular AP endonuclease and 3′-diesterase activities produce free 3′-hydroxyl groups required for DNA repair synthesis by DNA polymerases (13, 62).

Recent evidence suggests that protein-DNA interactions in chromatin are likely to influence the frequency, localization, and repair of DNA damage in vivo (31, 36, 49, 59, 65, 72). Progress toward understanding the relationships between distribution of DNA damage, DNA repair, and chromatin structure is severely dampened by the combined difficulty of quantifying DNA damage and assessing its relation to chromatin structure. The fact that the quantification of DNA damage is not an easy task is partly due to the large variety of lesions that can be induced, e.g., by ROS (15, 25). Several techniques are available to assess specific DNA lesions, including strand breaks (5, 37, 67, 73, 77), AP sites (32, 38, 81), and base or nucleotide modifications (15, 80, 82). Quantification of DNA strand breaks plus AP sites is usually achieved by alkaline unwinding (5, 67) or alkaline elution assays (37). However, none of these techniques is suitable to investigate the distribution of DNA damage along the genome. One recent approach based on ligation-mediated PCR was used with success to measure the relative frequency of UV-induced specific lesions (21, 60) and oxidative base damage (64) at nucleotide resolution in specific genes. This technique, however, is not suitable to assess both the average frequency and global distribution of DNA damage in the genome.

In the study reported here, we have used a combination of nucleases and DNA end labeling (i) to assess quantitatively the induction of DNA strand breaks and AP sites in mammalian

* Corresponding author. Mailing address: Santé et Environnement, Centre de Recherche du CHUL, 2705 Boulevard Laurier, Sainte-Foy, Québec, Canada G1V 4G2. Phone: (418) 656-4141, ext. 7097. Fax: (418) 654-2159. E-mail: memirault@crchul.ulaval.ca.

† Present address: Hôpital Maisonneuve Rosemont, Centre de Recherche, Montréal, Canada H1T 2M4.

cells exposed or not to different types of DNA-damaging agents and (ii) to analyze the distribution of these lesions in their genome. DNA end labeling was carried out by T4 DNA polymerase-mediated nucleotide exchange at 3′ ends in combination with the use of *E. coli* endonuclease IV to remove 3′ blocking groups and cleave AP sites. This 3′-end-labeling assay was chosen for quantification of DNA strand breaks and AP sites because the detection of single-strand breaks was found to be remarkably more efficient with T4 DNA polymerase than with terminal transferase (this study) or kinase to label 5′ ends resulting from oxidative damage. Earlier work had shown that most 5′ ends of DNA from irradiated cells could not be labeled by kinase, even after treatment with alkaline phosphatase (blocked 5′ termini) (12). In contrast, we show that the nucleotide exchange assay provides a powerful tool to monitor DNA damage and repair that occurred in cultured cells or in vivo. On the other hand, the genomic distribution of DNA damage resulting in single-strand breaks was investigated by use of the single-strand-specific S1 nuclease. Strikingly similar nonrandom patterns of S1 nuclease-mediated DNA cleavage were obtained with human cells and mice exposed to genotoxic agents, irrespective of the type of agent used. The simplest interpretation of our data suggests that the clustered distribution of single-strand breaks detected by S1 nuclease reflects primarily higher-order chromatin structure.

MATERIALS AND METHODS

Cell culture and treatments. The cell line T47D-Hygro-3 is a hygromycin B-resistant transfectant clone of human breast carcinoma T47D cells (54). Simian virus 40 (SV40)-transformed human WI38 fibroblasts (VA13), human fibroblasts (GM-1), and NIH 3T3 mouse fibroblasts were obtained from the American Type Culture Collection (Rockville, Md.). The human neuroblastoma cell line SK-N-BE(2)-M17 (9) was kindly supplied by J. Biedler. T47D-Hygro-3 cells were grown in RPMI 1640 medium as previously described (54), and the other cells were grown in Dulbecco modified Eagle medium. The media were supplemented with 10% fetal bovine serum (Gibco BRL, Grand Island, N.Y.), 2 g of sodium bicarbonate (Sigma, St. Louis, Mo.) per liter, 2 mM L-glutamine (Sigma), 0.1 μM sodium selenite (Sigma), 100 ng of insulin (bovine pancreas; Sigma) per ml, 100 U of penicillin (Gibco) per liter, and 0.1 mg of streptomycin (Gibco BRL) per liter. Cells were cultured in a humidified atmosphere in 5% CO_2 and at 37°C. For drug treatments, T47D-Hygro-3 cells were incubated at 37°C for 1 h in growth medium supplemented with menadione (Sigma), streptonigrin (Sigma), methylmethane sulfonate (MMS) (Sigma) or VM-26 (a generous gift from Bristol-Myers Co.) at the concentrations indicated in Results. The cells were then washed twice with cold phosphate-buffered saline (PBS) before lysis and DNA isolation. In gamma irradiation experiments, 50 to 70% confluent cells were exposed to ^{60}Co gamma rays at doses ranging from 0 to 500 Gy (116 rads/s) at 0°C (petri dish in ice-water bath). The cells were then lysed (see "DNA isolation" below) either immediately following exposure or after various periods of incubation at 37°C to allow DNA repair.

DNA isolation. Plasmid DNA was prepared by the sodium dodecyl sulfate (SDS)-alkali lysis procedure followed by banding in cesium chloride-ethidium bromide density gradients (68). Mammalian cell DNA was isolated by adding directly to 50 to 70% confluent cells in 100-mm-diameter petri dishes 2 ml of 1× lysis buffer containing 50 mM Tris-HCl (pH 7.4), 1% SDS, 20 mM EDTA, 10 μM deferoxamine mesylate (a chelator of Fe^{3+}) (Sigma), and proteinase K (0.5 mg/ml; Gibco BRL). After overnight digestion at 37°C in the petri dish, the viscous lysate was transferred into two Eppendorf tubes by using a Pipetman and wide-mouth 1-ml tips precut to minimize DNA shearing. Protein salting out was carried out as described by Miller et al. (53) by addition of 1/3 volume of saturated NaCl and efficient mixing. After centrifugation at 13,000 × *g* for 15 min at room temperature (RT), the DNA-containing supernatant was phenol extracted with 1 volume of phenol-chloroform saturated with NaCl, followed by chloroform extraction and ethanol precipitation by gentle mixing with 2 volumes of absolute ethanol at room temperature. The resulting DNA clot was immediately centrifuged down at 2,000 × *g* for 3 min. After being washed with 70% ethanol, the DNA pellet was resuspended overnight at 4°C in 0.4 ml of Tris-EDTA (TE) (per petri dish) without agitation and then gently shaken by hand intermittently and left for at least 2 days at 4°C for complete resuspension. The DNA precipitated in this way contained very little RNA (<5%). Note also that DNA samples were never vortexed and always treated so as to minimize physical shearing, nor were they dessicated (to avoid oxidation). Controls indicated that no relaxation of supercoiled Bluescript plasmid was detected after phenol extraction and isolation as described above, whether the plasmid was or was not treated with endonuclease IV before agarose gel analysis (42). Alternatively, cellular DNA was prepared in agarose plugs to avoid DNA manipulation and phenol extraction. Cells (1×10^5 to 1.5×10^5) were immobilized in 50-μl agarose plugs of 0.75% low-melting-point agarose (Bio-Rad) in PBS and incubated for 16 h at 50°C in 0.4 M EDTA (pH 7.8)–1% SDS–10 μM deferoxamine–0.5 mg of proteinase K per ml. The plugs were washed once in TE containing 10 μM deferoxamine (TED), twice in TED containing 1 mM phenylmethylsulfonyl fluoride to inactivate proteinase K, and twice in TED; each wash was for 1 h at 50°C in 5 ml. The DNA concentration (about 20 ng/μl in plugs) was measured with a TKO 100 DNA fluorometer according to the instructions of the manufacturer (Hoefer Scientific Instruments, Mississauga, Ontario, Canada). Extracted DNA and DNA plugs were stored at 4°C. The DNA was analyzed by field inversion gel electrophoresis (FIGE) according to the instructions of Hoefer Scientific Instruments, using 20-cm-long 1% agarose gels in Tris-borate-EDTA buffer, an electric field of 6.9 V/cm, a 28-h run time, a 1- to 50-s pulse time, and a forward/reverse ratio of 3.0:1 (Switchback pulse controller).

Mouse liver DNA was extracted from 1-, 6-, 12-, and 20-day-old and 2- to 3-month-old C57BL6 mice (Charles River Laboratories, Inc., Wilmington, Mass.). In some experiments, mice were injected with 200 mg each of cytosine arabinoside (AraC) and hydroxyurea (Sigma) in PBS per kg 6 h before sacrifice, in order to inhibit DNA synthesis. For induction of DNA damage in vivo, groups of three mice were injected intraperitoneally (i.p.) with 1.4 mmol of MMS (Sigma) per kg, or were not treated (controls), and sacrificed after 4 h. The mice were killed by cervical dislocation by methodology approved by the Canadian Council on Animal Care, and their livers were quickly removed and immediately placed in ice-cold TE (on ice). A piece of tissue (~50 mg) was homogenized with a potter glass frit at 0°C in 10 volumes of TE containing 10 μM deferoxamine mesylate. The homogenate was lysed by addition of 1 volume of 2× lysis buffer (see above) preheated to 50°C and was incubated at 37°C overnight. Protein salting out and phenol-chloroform extraction were carried out as described above. In some control experiments, cellular DNA was sheared extensively through a U-100 insulin syringe (1 ml; 29 gauge; 1/2 in.).

DNA 3′ end labeling. The DNA was 3′ end labeled by a nucleotide exchange reaction catalyzed by T4 DNA polymerase (7). DNA (200 ng) was incubated in a reaction mixture, freshly prepared, containing 33 mM Tris-acetate, 66 mM potassium acetate, 10 mM magnesium acetate (pH adjusted to 8.0), 0.5 mM dithiothreitol, 0.1 mg of bovine serum albumin per ml, 100 μM each dATP, dGTP, and dTTP, 0.165 μM [α-^{32}P]dCTP {DuPont NEN; 300 Ci/mmol (the 3,000-Ci/mmol stock of [α-^{32}P]dCTP was diluted 1:10 in 3.3 μM cold dCTP, and 1 μl was added to the incubation mixture}, and 0.5 U of T4 DNA polymerase (Pharmacia), in a final volume of 20 μl, for 1 h at 37°C. The reaction was stopped by heating for 5 min at 65°C. For determination of total radioactivity incorporated by dot filtration, 400 μl of AFPE buffer, containing 0.3 M ammonium formate, 0.1 M sodium pyrophosphate, and 1 mM EDTA (pH 7.8), was added at RT to each sample. Each DNA sample was then deposited on a preequilibrated NA-45 DEAE membrane (Schleicher & Schuell) or Hybond N^+ membrane (Amersham) on a Gibco BRL 96-well dot format (6-mm-diameter) Convertible Filtration Manifold System. All dots were rinsed four times with 400 μl of AFPE buffer, with the last rinse containing bromophenol blue for dot recognition. The whole membrane was then rinsed twice in AFPE buffer for 5 min. The blue dots were cut out, and radioactivity was measured by scintillation counting under the same conditions used to determine the specific radioactivity of the [α-^{32}P]dCTP (see below). Similar incorporation was obtained with different T4 DNA polymerase batches (Pharmacia Biotech Canada, Québec, Canada). The extent of nucleotide exchange was calculated from the specific activity of the radioactive nucleotide in the incubation mixture and the radioactivity (counts per minute) incorporated per nanogram of DNA. The specific activity of the radioactive nucleotide (counts per minute per millimole) was determined by scintillation counting of the radioactivity in 10 μl of a 1:100 dilution of the commercial stock of [α-^{32}P]dCTP (3,000 Ci/mmol). Similar extents of nucleotide exchange were obtained with 50 to 500 ng of DNA, and 10 times more radioactivity per nanogram of DNA could be incorporated when [α-^{32}P]dCTP (3,000 Ci/mmol) was not diluted by cold dCTP (see above). Under these conditions, one [α-^{32}P]dCp or less is exchanged at 3′ termini of 3′ recessed, 5′ recessed, or blunt ends, depending on the nucleotide sequence context (7). When indicated, the nucleotide exchange assay was carried out in the presence of 0.1 U of *E. coli* endonuclease IV added as the last reagent in the cocktail. Endonuclease IV was prepared by D.R. as previously described (46); 0.1 U of this enzyme is a large excess for 0.2 μg of DNA (46). Alternatively, DNA was 3′ end labeled by use of terminal deoxynucleotidyltransferase (terminal transferase) according to the instructions of the manufacturer (Boehringer, Mannheim, Germany), incorporating [α-^{32}P]ddCTP (DuPont NEN) under optimal conditions. The DNA samples were then processed as described above for radioactivity determinations. To label DNA in agarose plugs, 50 μl of plug and 50 μl of TE were melted for 10 min at 65°C and transferred to 37°C, and 20 μl (~0.2 μg of DNA) was incubated for 3′ labeling by nucleotide exchange as described above but in 40 μl. After addition of 160 μl of TE, the DNA was extracted with 1 volume of phenol-chloroform plus 1 volume of chloroform. The DNA concentration and radioactivity (by dot filtration) were determined as described above.

DNA 5′ end labeling. The number of 5′-hydroxyl-containing termini was determined by T4 polynucleotide kinase labeling of alkaline phosphatase- and alkali-treated DNA with [γ-^{32}P]ATP (68). Alkaline treatment of the DNA was carried out as described by Levin and Demple (45) to hydrolyze 5′-phosphate

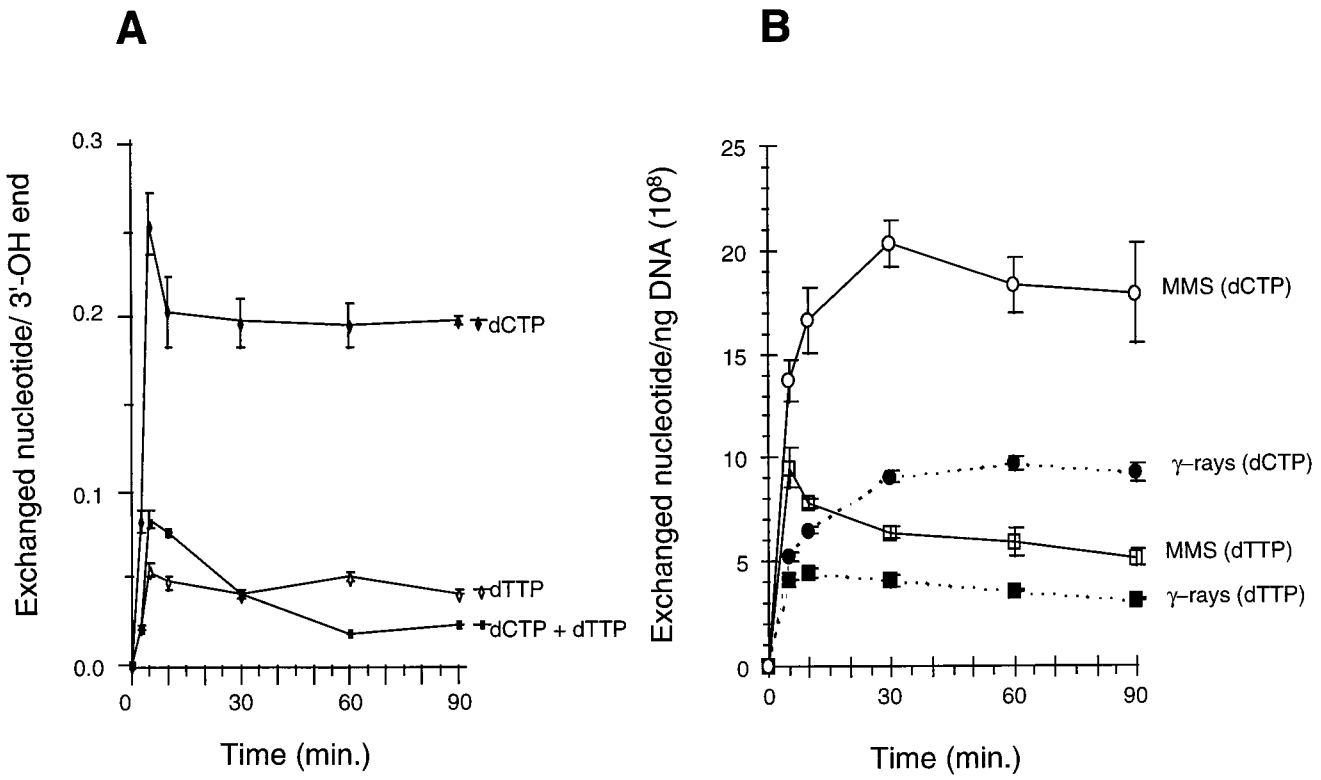

FIG. 1. Kinetics of nucleotide exchange catalyzed by T4 DNA polymerase. (A) Plasmid Bluescript KS digested with *Alu*I (32 3′ ends). (B) Damaged DNA isolated from T47D-Hygro-3 cells exposed to 100 Gy of gamma rays or 300 μM MMS for 1 h. T4 DNA polymerase-catalyzed nucleotide exchange at DNA 3′ ends was measured as described in Materials and Methods. Data are means ± standard deviations for three determinations (triplicate DNA preparations).

and 5′-deoxyribose-5-phosphate groups. Briefly, 2 μg of DNA was incubated for 45 min at 65°C in 40 μl of 0.2 M NaOH–10 mM EDTA and neutralized by addition of 40 μl of ice-cold 0.4 M Tris-HCl (pH 4.05). The DNA was precipitated with 2.5 volumes of ethanol for 30 min at −70°C. After centrifugation (20 min, 13,000 × *g*), the DNA was resuspended in 20 μl of TE (2 days at 4°C) and treated with 0.1 U of calf alkaline phosphatase per μg of DNA as described by the manufacturer (Pharmacia Biotech Canada). After heat inactivation of the phosphatase, 5′ end labeling of 0.1 μg of DNA was carried out with [γ-^{32}P]ATP (DuPont NEN) and T4 polynucleotide kinase for 45 min at 37°C as described by the manufacturer (Pharmacia Biotech Canada). After addition of EDTA to 25 mM, the DNA samples were treated with 1 U of RNase I or 1 U each of RNase A and RNase T_1 for 10 min at 65°C. This step ensures complete removal of any trace amount of RNA that would have resisted the first alkaline treatment and would be labeled together with DNA. The DNA samples were then processed as 3′-end-labeled DNA for radioactivity determinations (see above) and calculation of the number of phosphate groups incorporated per nanogram of DNA. In each experiment, *Eco*RI-digested plasmid Bluescript KS (0.1 μg) was used as a reference to calculate the yield of 5′ end labeling; this yield varied from 50 to 70% with freshly received [γ-^{32}P]ATP and was found to decrease with increasing decay of the radiolabeled nucleotide.

S1 nuclease treatment. DNA (1 μg) was incubated in 100 μl of S1 buffer containing 0.25 M NaCl, 0.05 M sodium acetate, 1 mM zinc acetate (pH 4.6), 0.05 mg of bovine serum albumin per ml, and 1 U of S1 nuclease (Pharmacia Biotech Canada) for 1 h at 15°C (not 37°C). The reaction was stopped by addition of 100 μl of 0.2 M Tris-HCl–50 mM EDTA (pH 8) followed by gentle phenol-chloroform extraction. The DNA was quantitatively precipitated by addition of 15 μl of 5 M NaCl and 2.5 volumes of cold absolute ethanol and refrigerated at −70°C for 30 min. The DNA was centrifuged at 13,000 × *g* for 15 min at 4°C and resuspended in TE after washing with 70% ethanol. The DNA was 3′ end labeled with T4 DNA polymerase as described above, incubated for 5 min at 65°C, and analyzed by conventional agarose gel electrophoresis overnight, using 20-cm-long 0.8% agarose gels in Tris-borate-EDTA buffer and a forward electric field of ~2 V/cm at RT. The gels were stained with ethidium bromide for visualization and dried under vacuum for autoradiographic exposure. Under the conditions described above, supercoiled plasmid Bluescript KS was resistant to cleavage by S1 nuclease (43).

RESULTS

DNA 3′ end labeling: comparison of T4 DNA polymerase-catalyzed nucleotide exchange with nucleotide extension by terminal deoxynucleotidyltransferase. Both terminal transferase (66) and bacteriophage T4 DNA polymerase (7, 54) have been used to label DNA 3′ ends. We had shown that the nucleotide exchange reaction catalyzed by T4 DNA polymerase at 3′ termini provides a convenient way to assess DNA strand breaks induced in cultured cells by an oxidant such as menadione, a quinone which generates O_2^- and H_2O_2 intracellularly by redox cycling (75) and induces DNA breaks in cultured cells (54); the observation that induction of these breaks can be prevented by transfection of glutathione peroxidase, a scavenger of H_2O_2, or by deferoxamine-mediated iron chelation strongly suggests hydroxyl or ferryl radical-mediated oxidative DNA damage (54, 55). On the other hand, terminal transferase-mediated 3′ end labeling (TUNEL assay) is currently used to detect internucleosomal DNA fragmentation associated with apoptosis (22, 23, 76). Experiments were thus designed to compare the relative efficiencies of both enzymes to label DNA isolated from human cells treated or not with DNA-damaging agents that produce predominantly single-strand breaks.

Experiments were first carried out to determine the optimal nucleotide exchange reaction conditions for maximal detection of 3′ ends in cellular DNA. Figure 1 shows the kinetics of nucleotide exchange that occurred with [α-^{32}P]dCTP or [α-^{32}P]dTTP as a labeled precursor in *Alu*I-cut plasmid Bluescript KS (Fig. 1A) and in damaged DNA isolated from cells exposed

to ionizing radiation or the alkylating agent MMS (Fig. 1B). The restriction enzyme *Alu*I was chosen to cut the plasmid DNA because it is a frequent cutter that generates blunt ends containing neither dC nor dT in 3′ (--AG$^{3'}$ termini), at which more than two nucleotides have to be removed to permit dC or dT exchange. As seen in Fig. 1, the maximal extent of average nucleotide exchange was obtained with labeled dCTP, with both plasmid and cellular DNAs. In contrast, the use of labeled dTTP (alone) or both dCTP and dTTP label yielded much lower exchange values. The lower extent of dTp exchange could reflect a steady-state condition in which dTp removal by T4 DNA polymerase 3′-exonucleolytic activity is more efficient than dCp removal with regard to polymerizing activity; the use of two labeled nucleoside triphosphates present at low concentrations in the reaction mixture further favors exonucleolytic versus polymerizing action of T4 DNA polymerase (7). The extent of dCp or dTp exchange reached a plateau within 5 to 10 min in *Alu*I-cut plasmid. In damaged cellular DNA, the maximal extent of dTp exchange was also reached within 5 to 10 min, while maximal dCp exchange was reached only after 30 to 60 min. As previously discussed by Challberg and Englund (7), the time required to reach steady-state labeling depends on the number of nucleotides which have to be removed. If so, the kinetics data obtained with cellular DNA (Fig. 2B) suggest that ionizing-radiation- and MMS-induced DNA strand breaks, mostly single-strand breaks (see below), occurred preferentially in AT-rich genomic DNA regions. The average dCp exchange per 3′ end of single-strand breaks was measured in supercoiled plasmids nicked with DNase I or partially depurinated at acidic pH and cleaved with endonuclease IV to produce one nick per plasmid: the calculated dCp exchange was 0.25 in pBluescript KS and 0.89 in a plasmid containing a human gene (*hsc70* [16]). In genomic DNA, an average dCp exchange value ranging from 0.4 to 1.0 was estimated with DNAs isolated from various mouse tissues and cultured human cells, based on the number of 5′ ends determined by kinase assay (see below). As discussed previously (7), the rate and extent of nucleotide exchange depend on the base composition and nucleotide sequence (e.g., see labeled λ fragment markers in Fig. 7, 8, and 10) (data not shown). In view of the kinetics results obtained with cellular DNA, standard nucleotide exchange assay conditions were set for 60 min at 37°C with [α-^{32}P]dCTP as a radioactive precursor (see Materials and Methods).

Figure 2 shows a comparison of the relative efficiencies of T4 DNA polymerase and terminal transferase in labeling DNA isolated from human cells incubated for 1 h with the oxidant menadione or the methylating agent MMS to induce DNA strand breaks. As shown in Fig. 2, the incorporation of [α-^{32}P]dCTP by T4 DNA polymerase was much more efficient than that of [α-^{32}P]ddCTP by terminal transferase (single ddCp extensions) in both menadione- and MMS-damaged cellular DNA. In contrast, the labeling efficiencies were similar at the ends of bacteriophage λ DNA, which provides a positive control for the terminal transferase reaction. The difference in labeling efficiency observed with the cellular DNAs was unlikely to be due to multiple dCp exchange per 3′ end by T4 DNA polymerase as opposed to single ddCp extension by terminal transferase, since (i) an average of one labeled nucleotide or fewer (dCp or dTp) was found to be exchanged by T4 DNA polymerase at both double-strand and single-strand breaks and (ii) similar extents of labeling were obtained with λ DNA with the two enzymes (Fig. 2). Therefore, the data shown in Fig. 2 indicate that many more strand breaks, presumably nicks and gaps, are detected by T4 DNA polymerase end labeling than by terminal transferase end labeling, with both

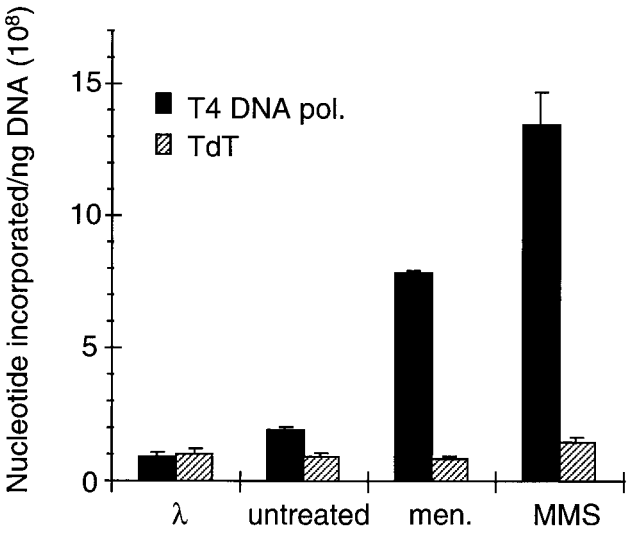

FIG. 2. Comparison of 3′ end labeling with T4 DNA polymerase or terminal deoxynucleotidyl transferase. Proliferating T47D-Hygro-3 cells were untreated (control) or treated for 1 h with 150 μM menadione (men.) or 300 μM MMS. Phage λ DNA (heat treated to melt cohesive ends) and cellular DNAs were 3′ end labeled by T4 DNA polymerase (pol.)-catalyzed nucleotide exchange with [α-^{32}P]dCTP (black bars) or by terminal deoxynucleotidyl transferase-mediated (TdT) single-nucleotide extension with [α-^{32}P]ddCTP (hatched bars). Both labeled precursors had the same specific radioactivity. Incorporated radioactivity was measured by DNA dot filtration (see Materials and Methods). Data are means ± standard deviations for three determinations (triplicate DNA preparations).

enzymes being used under optimal conditions. The nucleotide exchange assay was thus chosen to monitor 3′ ends in cellular DNA.

Basal levels of 3′ and 5′ ends detected in cellular DNA by end-labeling assays. Quantification of DNA strand interruptions and breaks in cells exposed to any DNA-damaging agent, measured by any technique, is inevitably assessed over a basal level (background) of strand interruptions present in DNA of unexposed cells. Various factors will contribute to this background, including normal DNA metabolism (e.g., replication and transcription), basal DNA damage and repair, and damage introduced during DNA isolation. The background of nucleotide exchange catalyzed by T4 DNA polymerase at 3′ ends was first determined for DNAs isolated from various cell lines grown under normal conditions. As shown in Table 1, the average basal level of dCp exchange ranged from a low of 1.44×10^8 dCps/ng of DNA in mouse NIH 3T3 cells to 2.35×10^8 dCps/ng of DNA in human SK-N-BE(2)-M17 neuroblastoma cells, as measured in the same experiment under proliferative conditions. This corresponds to a frequency of 0.15 to 0.25 3′-hydroxyl-containing 3′ end per kb of DNA, on average, i.e., regardless of the distribution of DNA strand interruptions. Interestingly, the basal level of dCp exchange was about twofold lower in confluent cells (e.g., compare results for T47D-Hygro-3 cells in Table 1 and Fig. 3B), suggesting that DNA replication and metabolism contributed an important fraction of the DNA 3′ ends detected (see below). Besides, inclusion of endonuclease IV (in excess) in the assay to hydrolyze AP sites and 3′-blocked termini increased the dCp exchange to small extents that ranged from a nonsignificant 6% in SK-N-BE(2)-M17 cells to a significant 23% increment in WI38-VA13 cells (Table 1).

The average basal level of dCp exchange was also determined for DNAs prepared from several mouse tissues imme-

TABLE 1. Basal levels of T4 DNA polymerase-catalyzed dCp exchange in DNAs of various cell lines[a]

Cell line	Exchanged dCps/ng DNA (10^8)[b]		P (Student t test)[c]
	Without endonuclease IV	With endonuclease IV	
T47D-Hygro-3	1.71 ± 0.13	2.03 ± 0.14	0.0003
WI38-VA13	1.82 ± 0.20	2.23 ± 0.24	0.002
GM-1	1.77 ± 0.10	1.95 ± 0.15	0.03
NIH 3T3	1.44 ± 0.05	1.66 ± 0.03	0.003
SK-N-BE(2)-M17	2.35 ± 0.10	2.48 ± 0.20	0.13

[a] DNA isolated from proliferating cells was 3′ end labeled with T4 DNA polymerase, in the absence or presence of endonuclease IV, with [α-^{32}P]dCTP as a radioactive precursor. The incorporated radioactivity was measured by dot filtration and converted into number of dCps exchanged per nanogram of DNA (see Materials and Methods).

[b] Means ± standard deviations for three determinations.

[c] Statistical significance of the difference between the values obtained in the presence and absence of endonuclease IV.

diately after dissection. Table 2 lists the results obtained with single healthy 8-week-old C57BL/6 mice in different experiments (independent assays). As can be seen in Table 2, the basal level of dCp exchange in the various tissues investigated ranged from low levels close to those found in cultured cell lines, i.e., around 1.5×10^8 to 2.5×10^8 dCps/ng of DNA (without endonuclease IV), to higher levels such as those found in muscle, heart, brain, and skin. The data obtained with three samples of tissue excised from each of three individual mice ($n = 9$) indicate a very good reproducibility of dCp exchange measurements in most tissues and little variability among different individuals (e.g., see Fig. 5). With all tissues investigated, inclusion of endonuclease IV in the assay increased the nucleotide exchange by 10 to 20%, except in cortex, where the increment was very reproducibly higher (36% on average). This unusual increment suggests frequent oxidative DNA damage in mouse cortex (see Discussion). Two kinds of experiments were carried out to assess the contribution of normal DNA metabolism, including DNA synthesis, to the basal level of 3′ ends detected. First, one group of three mice received 200 mg of AraC per kg and 200 mg of hydroxyurea per kg (i.p.) 6 h before sacrifice in order to inhibit DNA synthesis (18), to be compared with a second group of three untreated animals (controls). In liver DNA of AraC-hydroxyurea-treated mice, the extent of nucleotide exchange was reduced by an average of 37% (38.5% with endonuclease IV). In kidney, this reduction was 31% (35% with endonuclease IV). Second, the basal level of 3′ ends was also determined in tissues documented to have elevated DNA synthesis, such as skin and liver at early stages of postnatal development. Such tissues showed elevated levels of nucleotide exchange (Table 2). Thus, not surprisingly, all of these results indicate that DNA synthesis may contribute a significant part of the 3′ ends detected in proliferating cells.

Artifactual DNA breaks introduced during DNA isolation can result from chemical damage, e.g., oxidation during phenol extraction, and from physical shearing inevitably associated with DNA manipulation. Three types of experiments were carried out to assess the contribution of DNA damage introduced during DNA extraction and isolation to the basal 3′ end labeling observed. Figure 3A and B show the results of an experiment in which the extents of DNA breakage and 3′ end labeling were compared for cellular DNA isolated by phenol extraction or prepared from cells immobilized in agarose plugs, i.e., without phenol extraction and DNA manipulation (see Materials and Methods). Double-strand breaks were assessed by FIGE in proliferating T47D-Hygro-3 cells exposed, or not (control), to menadione (150 μM, 1 h) to induce breaks of oxidative origin. DNA breakage caused by the extraction procedure is clearly evident in unexposed control cells: the DNA size was reduced from >500 kb in agarose plugs to about 100 to 300 kb after phenol extraction and isolation (Fig. 3A). In contrast, however, no significant difference in the extent of T4 DNA polymerase-mediated 3′ end labeling was detected (Fig. 3B). Similarly, with menadione-damaged DNA, no difference in 3′ end labeling between the two DNA isolation procedures was detected (Fig. 3B), although the weight-average size of the extracted DNA was evidently smaller than that of agarose plugs (Fig. 3A). These results indicate (i) that the 3′ ends of physical double-strand breaks introduced during DNA isolation are not suitable substrates for T4 DNA polymerase-catalyzed nucleotide exchange (probably not 3′-hydroxyl termini) and (ii) that our phenol extraction procedure did not induce significant strand breakage during DNA isolation. To further verify the former suggestion, isolated cellular DNA was sheared extensively through a syringe needle, reducing its size from >100 kb to 5 to 10 kb (weight average) (Fig. 3C, inset). Both experimentally sheared and unsheared DNAs were 3′ end labeled in the presence or absence of endonuclease IV. Figure 3C shows that a massive introduction of physical double-strand breaks, corresponding to a 10- to 20-fold increase in 3′ ends, enhanced dCp exchange only 0.6-fold, irrespective of endonuclease IV treatment. This second result thus confirms

TABLE 2. Basal levels of T4 DNA polymerase-catalyzed dCp exchange in DNAs of various mouse tissues[a]

Tissue and age of mice[b]	Exchanged dCps/ng DNA (10^8) (mean ± SD)		n[c]
	Without endonuclease IV	With endonuclease IV	
Kidney	1.58 ± 0.51	1.95 ± 0.68	9
Liver	1.92 ± 0.57	2.34 ± 0.72	9
Thymus	2.48 ± 0.78	2.94 ± 1.04	9
Lung	2.56 ± 0.78	2.96 ± 0.99	9
Pancreas	2.62 ± 0.36	3.12 ± 0.44	9
Spleen	2.88 ± 1.17	3.47 ± 1.43	9
Testicle	3.26 ± 1.09	3.74 ± 1.37	9
Muscle	4.45 ± 0.78	5.08 ± 0.86	9
Heart	5.37 ± 0.67	6.12 ± 0.89	9
Cortex	13.04 ± 2.12	17.67 ± 2.62	9
Cerebellum	14.81 ± 2.34	17.53 ± 0.61	3
Skin	18.62 ± 6.18	20.36 ± 5.98	9
Liver			
1 day			
Mouse 1	4.92 ± 0.96	6.20 ± 1.21	3
Mouse 2	5.46 ± 0.83	7.05 ± 0.79	3
6 days			
Mouse 1	4.01 ± 0.92	4.53 ± 1.16	3
Mouse 2	3.36 ± 0.33	3.79 ± 0.24	3
12 days			
Mouse 1	1.59 ± 0.14	1.82 ± 0.15	3
Mouse 2	1.47 ± 0.22	1.93 ± 0.51	3
20 days			
Mouse 1	0.92 ± 0.25	1.62 ± 0.15	3
Mouse 2	1.24 ± 0.24	1.58 ± 0.26	3

[a] Exchanged dCp in DNAs isolated from various mouse tissues, including livers of developing young mice, was determined as described for Table 1.

[b] Tissues were from adult mice unless otherwise indicated.

[c] $n = 9$ means three mice and three tissue samples per mouse.

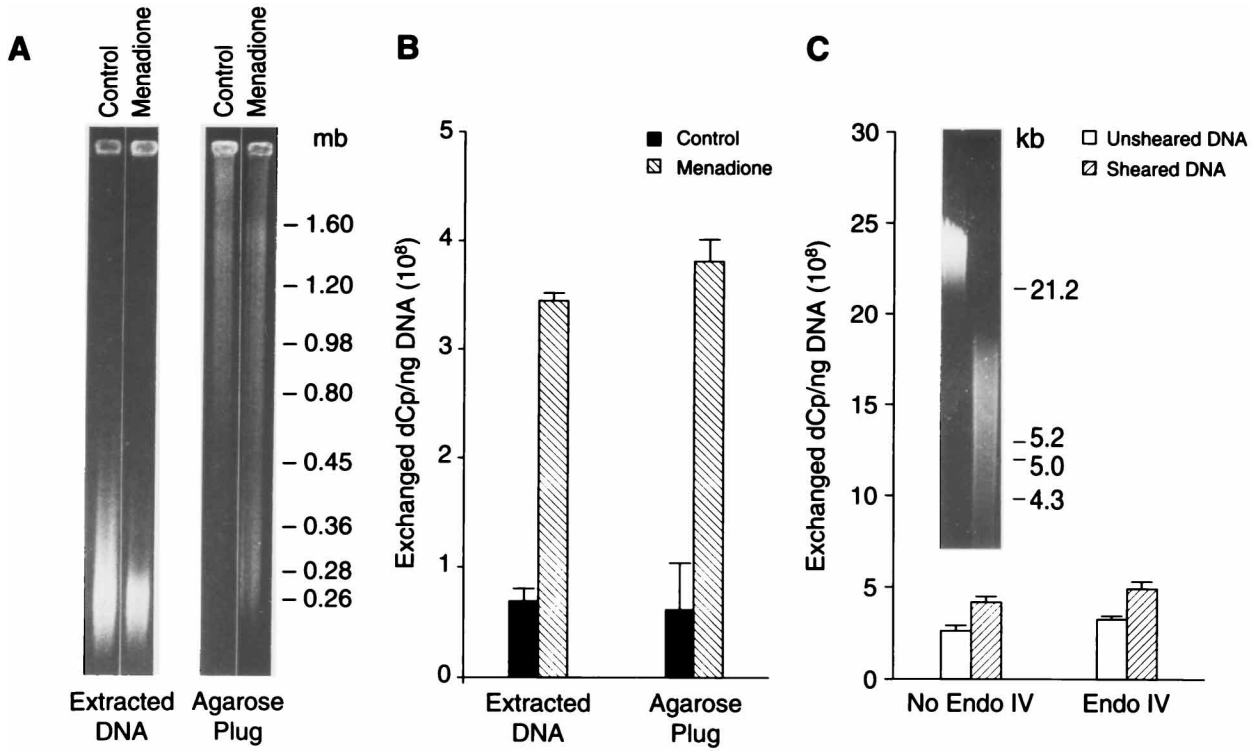

FIG. 3. Negligible contribution of DNA isolation and mechanical shearing to determinations of 3′-end frequency by nucleotide exchange. (A and B) Confluent T47D-Hygro-3 cells were exposed or not (control) to 150 μM menadione for 1 h. One part of each was processed for DNA isolation, including phenol extraction, and another part was immobilized in agarose plugs for DNA preparation in the absence of manipulation and phenol extraction (see Materials and Methods). (A) DNA analyzed by FIGE (6.9 V/cm, 1 to 50 s). Ethidium bromide staining is shown. (B) 3′-end-labeling dCp exchange is shown. Data are means ± standard deviations for three determinations (triplicate DNA preparations). (C) Total cellular DNA was isolated from proliferating T47D-Hygro-3 cells. Mechanically sheared and unsheared DNAs were analyzed by FIGE (10 V/cm, 1 to 20 s) (inset, ethidium bromide staining) and for dCp exchange in the presence or absence of endonuclease IV. Data are means ± standard deviations for three determinations (triplicate DNA preparations).

our first conclusion that physical strand breaks introduced during DNA isolation did not contribute significantly to the number of 3′ ends detected in untreated cells or tissues by the nucleotide exchange assay. Finally, experiments assessing the resistance of supercoiled plasmid DNA to relaxation induced by endonuclease IV after phenol extraction and isolation performed exactly as with cellular DNA showed that DNA cleavage possibly associated with phenol extraction contributed less than 1% of the total dCp exchange measured in cellular DNA (43). Therefore, altogether, the control experiments indicate three things: (i) virtually all basal 3′ termini detected in isolated cellular DNA by nucleotide exchange preexisted in the cells before DNA isolation; (ii) the physical double-strand breaks introduced during DNA isolation are not efficiently labeled by T4 DNA polymerase-catalyzed nucleotide exchange; and (iii) the majority of 3′ end structures generated by physical breaks can apparently not be processed by endonuclease IV to produce substrates suitable for T4 DNA polymerase exonucleolytic action.

For the sake of quantification, the basal number of dCps exchanged at 3′ ends plus cleaved AP sites determined in the nucleotide exchange assay (with endonuclease IV) was compared to the number of phosphates added at 5′ ends by polynucleotide kinase (kinase assay). Kinase labeling was carried out after alkaline and phosphatase treatments of the DNA to hydrolyze AP sites and resulting 5′-deoxyribose-5-phosphate groups and to remove 5′-phosphates. After correction for the kinase labeling efficiency determined in the same experiment (see Materials and Methods), the comparison was made for several mouse tissues, yielding the following results: liver, $(3.09 \pm 0.10) \times 10^8$ dCps/ng of DNA versus $(2.96 \pm 0.09) \times 10^8$ 5′ ends/ng of DNA; kidney, $(1.34 \pm 0.25) \times 10^8$ dCps/ng of DNA versus $(3.31 \pm 0.37) \times 10^8$ 5′ ends/ng of DNA; and thymus, $(2.48 \pm 0.20) \times 10^8$ dCps/ng of DNA versus $(3.27 \pm 0.63) \times 10^8$ 5′ ends/ng of DNA. Corresponding determinations made with DNA isolated from normally growing human cells (T47D-Hygro-3) yielded similar dCp exchange values, i.e., $(2.03 \pm 0.14) \times 10^8$ dCps/ng of DNA versus $(2.57 \pm 0.14) \times 10^8$ 5′ ends/ng of DNA. Thus, the number of DNA strand interruptions determined by 3′-end nucleotide exchange is in very good agreement with that determined by 5′ end labeling in the kinase assay. An average value of 0.7 dCp exchanged per 3′ end can be calculated from these data; the values ranged from 0.4 to 1.0 in human and mouse DNAs. These values are in excellent agreement with the direct determinations obtained with plasmid DNA models (see above). Finally, changing the sequence context at 3′ ends of cellular DNA by progressive exonucleolytic trimming with T4 DNA polymerase had no significant effect on the average dCp exchange determinations and thus on the quantification of 3′-hydroxyl-containing termini (data not shown).

Distinct patterns of DNA damage induced by different types of clastogenic agents. 3′ end labeling was used in combination with endonuclease IV to analyze quantitatively DNA damage of various origins in both cultured human cells and live mice. Figure 4 shows distinct examples of DNA damage and repair patterns induced in T47D-Hygro-3 cells. In these experiments, cells were incubated for 1 h with increasing concentrations of

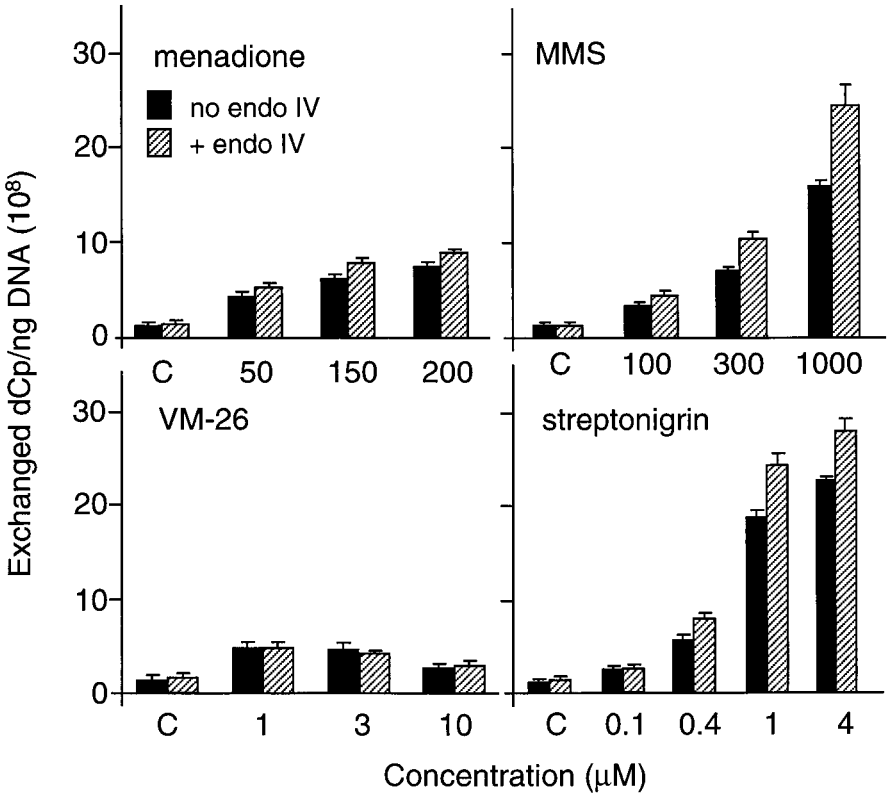

FIG. 4. Comparison of DNA damage patterns induced in human cells by different types of clastogenic agents. Proliferating T47D-Hygro-3 cells were exposed to MMS, menadione, or the topoisomerase II inhibitors VM-26 and streptonigrin, as described in Materials and Methods. Total cellular DNA was isolated and 3′ end labeled with T4 DNA polymerase and [α-^{32}P]dCTP in the presence (hatched bars) or absence (black bars) of endonuclease IV. The average extent of dCp exchange was measured by DNA dot filtration and calculated from the radioactivity incorporated (see Materials and Methods). Data are means ± standard deviations for three determinations (triplicate DNA preparations).

a specific genotoxic agent before DNA isolation, a situation where DNA damage and repair may occur concomitantly. The resulting "steady-state" damage in cellular DNA was analyzed by nucleotide exchange assay in the absence or presence of endonuclease IV to reveal AP sites and 3′-blocked termini in addition to 3′-hydroxyl-containing strand breaks.

The top left panel of Fig. 4 shows the dose-dependent effect of menadione on DNA damage induced in 1 h. Nucleotide exchange measured in the absence of endonuclease IV monitors 3′-hydroxyl-containing strand breaks, the most common DNA repair intermediate. Inclusion of endonuclease IV in the labeling assay was found to enhance nucleotide exchange by 20 to 30% in menadione-treated cells (with the background of control cells subtracted). This labeling enhancement is likely to reflect removal of 3′-blocking phosphates and phosphoglycolates typically produced by oxidative damage and cleavage of AP sites, including "oxidized" AP sites (27).

The specific detection of regular AP sites was tested by exposing cells to the methylating agent MMS. The most frequent DNA lesions detected in MMS-treated cells include AP sites and transient single-strand breaks containing 3′-hydroxyl termini (62). In mammalian cells, the majority of these strand breaks are thought to result from class II AP endonuclease-mediated cleavage of AP sites (45). As shown in the top right panel of Fig. 4, MMS induced a concentration-dependent increase of 3′ ends. In this case, the label increment produced by endonuclease IV provides a quantitative estimate of unprocessed AP sites. These sites accounted for a 52 to 57% label increment over the whole range of MMS concentrations used (0.1 to 1 mM). Thus, after 1 h of exposure to MMS, about 35% of the DNA lesions detected in the presence of endonuclease IV (with the background of untreated cells subtracted) were AP sites and 65% were single-strand breaks. A similar ratio was observed in mouse NIH 3T3 cells treated in the same way (data not shown). This ratio varied somewhat in different experiments, sometimes reaching up to 1:1 in cultured cells. It corresponds to a steady-state ratio of about one AP site for one to two strand breaks, a ratio thought to result from the simultaneous occurrence of DNA damage and DNA repair. If the 2- to 3-min half-life of rapidly repaired single-strand breaks observed after gamma irradiation (see Fig. 9) was similar in MMS-treated cells, the half-life of AP sites would thus be on the order of 1 to 2 min in these cells. Figure 5 shows an example of DNA damage quantification in liver and kidney DNAs of adult mice treated i.p. with MMS for 3 h. Note the reproducibility of the measurements and a significant variability among some individuals. For example, the extents of MMS-induced strand breakage (dCp exchange, no endonuclease IV) and levels of AP sites (increments of dCp exchange, with endonuclease IV) were significantly higher in both tissues of mouse 4 than in mice 5 and 6 (Fig. 5). The average extent of damage observed in mouse liver roughly corresponds to that observed in human cells exposed to 300 μM MMS for 1 h (Fig. 4). For the purpose of absolute quantification, the total number of AP sites plus single-strand breaks induced by MMS was also assessed by 5′ end labeling in the kinase assay (see Ma-

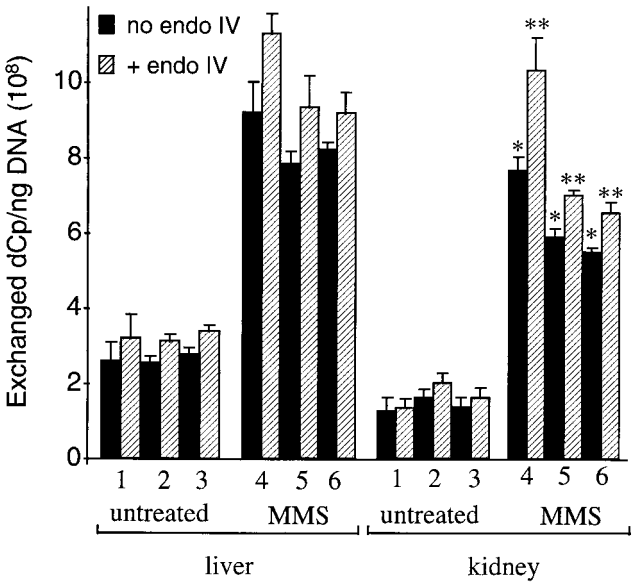

FIG. 5. Basal levels of 3′ ends and DNA damage patterns determined in mouse tissues. dCp exchange was measured in liver and kidney DNAs of adult mice treated or not with MMS. The average extent of dCp exchange was calculated as described for Fig. 4. Data are means ± standard deviations for three determinations (triplicate DNA preparations). Different mouse individuals were numbered 1 to 6. dCp exchange in kidney DNA of mouse 4 was significantly different than those in mice 5 and 6 (*, no endonuclease IV, $P < 0.05$; **, endonuclease IV, $P < 0.05$ [analysis of variance by the Newman-Keuls test]).

terials and Methods). For example, in mouse liver DNA, the average number of phosphates incorporated at 5′ ends after AP site hydrolysis was $(9.64 \pm 1.7) \times 10^8$/ng of DNA (mouse 5 in Fig. 5) after subtraction of basal 5′-end levels determined in liver DNA of control mice and correction for kinase labeling efficiency (see Materials and Methods). This value is in the same range as the number of dCps exchanged in the 3′-end-labeling assay with endonuclease IV, i.e., $(6.20 \pm 0.53) \times 10^8$ dCps/ng of DNA (same DNA). These data indicate an average frequency of 0.7 to 1 lesion, strand break, or AP site per kb of DNA, regardless of lesion distribution, which was found to be highly nonrandom (see below).

The nonintercalative antitumor drug VM-26, a topoisomerase II inhibitor of the epipopodophyllotoxin class, cleaves DNA through stabilization of a cleavable complex formed between topoisomerase II and DNA (8). Such cleavage generates 3′-hydroxyl-containing termini (suitable for 3′ end labeling) and blocked 5′ ends with a covalently linked topoisomerase II subunit (48). The nucleotide exchange assay was used to quantify DNA strand breaks induced in T47D-Hygro-3 cells by increasing concentrations of VM-26. As shown in Fig. 4, a concentration of 1 μM VM-26 was sufficient to produce maximal DNA cleavage in these cells. Of interest, at the higher concentration of 10 μM VM-26, the extent of nucleotide exchange was about half of that observed at 1 μM. Although the basis for this decrease is not clear, it could be associated with inhibitory effects of the drug on replication and transcription, leading to a decrease of basal dCp exchange. On the other hand, as expected, inclusion of endonuclease IV in the assay had no effect on the extent of 3′ end labeling obtained. This result also demonstrates that the endonuclease IV treatment per se did not induce any detectable increase in 3′ ends.

In contrast to the results with VM-26, a different and more complex pattern of DNA damage was obtained with another topoisomerase II inhibitor, streptonigrin. This drug is a potent nonintercalative topoisomerase II inhibitor (83) and also a potential hydroxyl radical generator (28). At a low concentration of streptonigrin (0.1 μM), as with VM-26, nucleotide exchange was not enhanced by endonuclease IV treatment (Fig. 4). At this concentration, streptonigrin apparently acted as a bona fide topoisomerase II inhibitor. In contrast, at 0.4 μM and higher concentrations, streptonigrin clearly induced more strand breaks than VM-26. The pattern of nucleotide exchange enhancement produced by endonuclease IV was similar to that observed with menadione, suggesting predominant oxidative DNA damage at high concentrations of streptonigrin. Up to 50% of the DNA damage inflicted by 0.4 μM streptonigrin could be inhibited by preincubating the cells in the presence of 100 μM deferoxamine added 2 h before drug addition (42), thus suggesting partial involvement of an iron-dependent oxidative mechanism, as found in bacteria (11). By comparison, up to 94% of comparable levels of DNA damage could be suppressed by deferoxamine in menadione-treated cells, suggesting that DNA damage induced by this quinone was almost exclusively of oxidative origin and iron dependent (42).

Differential quantification of ionizing-radiation-induced DNA strand breaks containing 3′-hydroxyl and 3′-blocked termini. Studies of DNA damage induced in cells exposed to ionizing radiation, e.g., gamma rays, offer the double advantage that (i) "initial" damage inflicted at 0°C can be assessed before cellular DNA gets repaired, and (ii) kinetics of postradiation DNA repair can be measured in cells further incubated at 37°C, in the absence of irradiation (see below). The major lesions found in DNA isolated from gamma-irradiated cells include single-strand breaks, oxidized bases, and AP sites (78). 3′-hydroxyl-containing termini can be directly assessed by T4 DNA polymerase-mediated 3′ end labeling in the absence of endonuclease IV; parallel end labeling carried out in the presence of this endonuclease measures the sum of 3′-hydroxyl and 3′-blocked termini and AP sites cleaved in the assay. The gamma radiation dose-dependent formation of these lesions was measured in this way in proliferating human T47D-Hygro-3 cells irradiated at 0°C at doses ranging from 0 to 500 Gy. Irradiation periods were very short (<3 min) in order to minimize any possible DNA repair at 0°C. DNA was isolated immediately afterward. As shown in Fig. 6A, the extent of nucleotide exchange was linearly related to the dose of gamma radiation up to 200 Gy, as observed in several experiments. At higher radiation doses, however, the increase in dCp exchange was no longer linear (Fig. 6B). The slope of the linear regression obtained between 0 and 200 Gy (experiment of Fig. 1A) in the absence or presence of endonuclease IV yielded, respectively, 1.70×10^6 ($r^2 = 0.99$) and 3.05×10^6 ($r^2 = 0.99$) dCps/ng of DNA/Gy. Note that about 55 to 65% (depending on the dose and experiment) of the lesions detected did not require endonuclease IV processing in order to be labeled by T4 DNA polymerase immediately after irradiation in ice and were thus presumably 3′-hydroxyl-containing termini (see also Fig. 9A, $t = 0$). The total frequency of single-strand breaks plus AP sites deduced from the linear regression data would be 4.3×10^{-3} lesion detected per kb per Gy, using an average dCp exchange per 3′ end of 0.7. The observation that the majority of gamma ray-induced strand breaks contained 3′-hydroxyl groups contrasts with previous reports that >95% of 3′ termini of naked DNA irradiated in vitro contain 3′ blocking groups that prevent action of T4 DNA polymerase (29, 30) (see Discussion). We therefore tested the possibility that the presence of 3′-hydroxyl groups in irradiated cells could reflect very rapid DNA repair occurring at 0°C during the time of irradi-

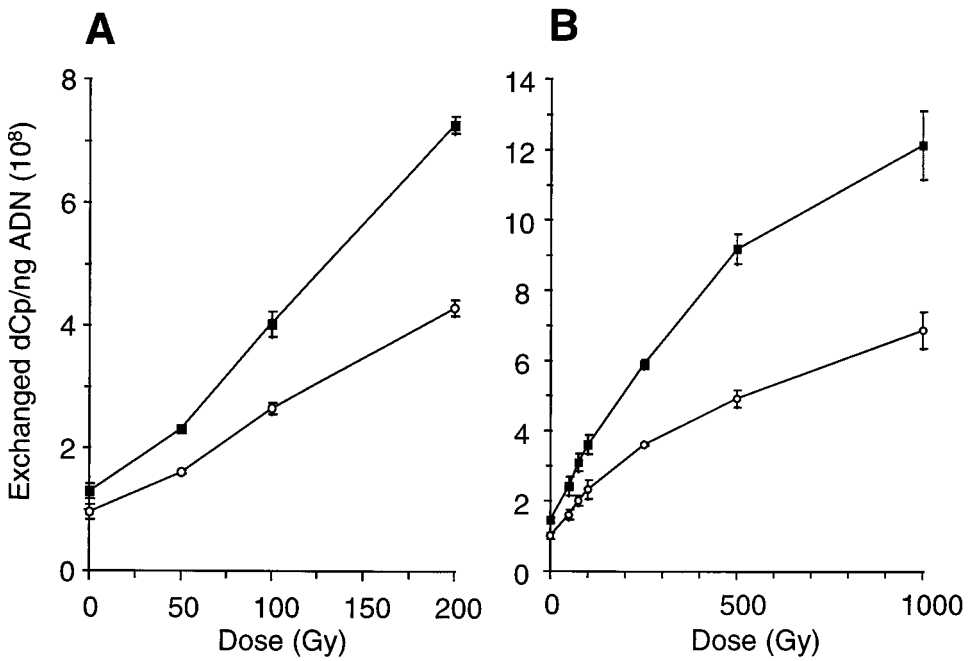

FIG. 6. 3′-Hydroxyl and 3′-blocked termini at DNA strand breaks induced in gamma-irradiated cells. T47D-Hygro-3 cells were exposed on ice to increasing doses of gamma irradiation. (A) 0 to 200 Gy; (B) 0 to 500 Gy. Total cellular DNA was isolated and 3′ end labeled with T4 DNA polymerase and [α-^{32}P]dCTP, in the presence (filled squares) or absence (open circles) of endonuclease IV. The average extent of dCp exchange was measured by DNA dot filtration and calculated from the radioactivity incorporated. Data are means ± standard deviations for three determinations (triplicate DNA preparations).

ation and cell transfer for DNA isolation (maximum of 2 to 4 min). Such repair, however, was very unlikely since neither the total dCp exchange measured in the presence of endonuclease IV nor the endonuclease IV-mediated labeling increment decreased during 5 or even 60 min postincubation at 0°C (data not shown).

Chromatin structure, not DNA sequence, is the primary determinant of S1 nuclease-hypersensitive site formation in response to ionizing radiation. The genomic distribution of gamma ray-induced DNA strand interruptions was investigated by use of the single-strand-specific nuclease S1. DNA from T47D-Hygro-3 cells exposed to 100 Gy at 0°C was treated or not with S1 nuclease under stringent conditions (high salt, 15°C [see Materials and Methods]) before 3′ end labeling and agarose gel electrophoresis. It should be emphasized that, under the incubation conditions used, both supercoiled and DNase I-relaxed Bluescript KS plasmids were relatively resistant to S1 nuclease cleavage; in contrast, single-stranded gaps of several nucleotides were efficiently cleaved (43). Figure 7A and B show the time-dependent cleavage of this DNA by S1 nuclease at 15°C. The cleavage patterns observed in the autoradiogram of Fig. 7B suggest two distinct effects of S1 nuclease. First, there was a rapid cleavage of hypersensitive sites that was essentially completed within 30 min of incubation and produced small S1 fragments ranging from about 0.5 to 2 kb, in addition to large, >50-kb DNA fragments (not resolved). In contrast to the >50-kb DNA band visible in Fig. 7A, the small fragments detected by autoradiography in Fig. 7B escaped detection by ethidium bromide staining. These fragments accounted for at most 1% of the total DNA, as measured by diphenylamine assay in large-scale experiments. Second, we also observed a much slower process detected between 30 and 90 min, which produced a progressive decrease in the size of the small S1 fragments, with no concomitant increase in global 3′ end labeling (Fig. 7C) and thus no further S1 endonucleolytic cleavage. The rate of this progressive fragment shortening was considerably higher when S1 digestion was carried out at 37 instead of 15°C (data not shown). The strong temperature dependence of this effect suggests an exonucleolytic action of S1 on easily melted DNA ends, e.g., nibbling of "breathing" DNA ends with very AT-rich composition. The most striking observation in Fig. 7B is the fast kinetics component, which shows rapid cleavage at S1-hypersensitive sites. The approximate doubling of radioactivity incorporated in S1-treated DNA at the plateau level (30 to 60 min versus time zero in Fig. 7C) supports the view that the vast majority of S1-hypersensitive sites induced by gamma rays are strand gaps, since each strand cleavage mediated by S1 nuclease at these sites generates a second 3′ end accessible for labeling. It should be noted that a basal level of S1 cleavage was also observed in DNA from control unirradiated cells (Fig. 7B and C), although the yield of S1 fragments produced was low to very low depending on cell type and varied somewhat from experiment to experiment (e.g., compare results in Fig. 7B, 8B, and 10). The S1 nuclease cleavage data suggest (i) that the majority of the gamma ray-induced DNA strand breaks detected were clustered in unknown regions of cellular DNA and (ii) that a similar distribution of DNA strand interruptions preexisted at a much lower frequency in nonirradiated cells. Moreover, these S1 fragments derived from the nuclear genome, since a possible mitochondrial origin could be ruled out by Southern blot hybridization data (not shown).

An experiment was then performed to find out whether the observed distribution of S1-hypersensitive sites was determined primarily by DNA sequence or chromatin structure. Figure 8 shows a comparison of S1 nuclease cleavage patterns obtained with DNA extracted from cells exposed to increasing doses of gamma radiation with the patterns obtained with

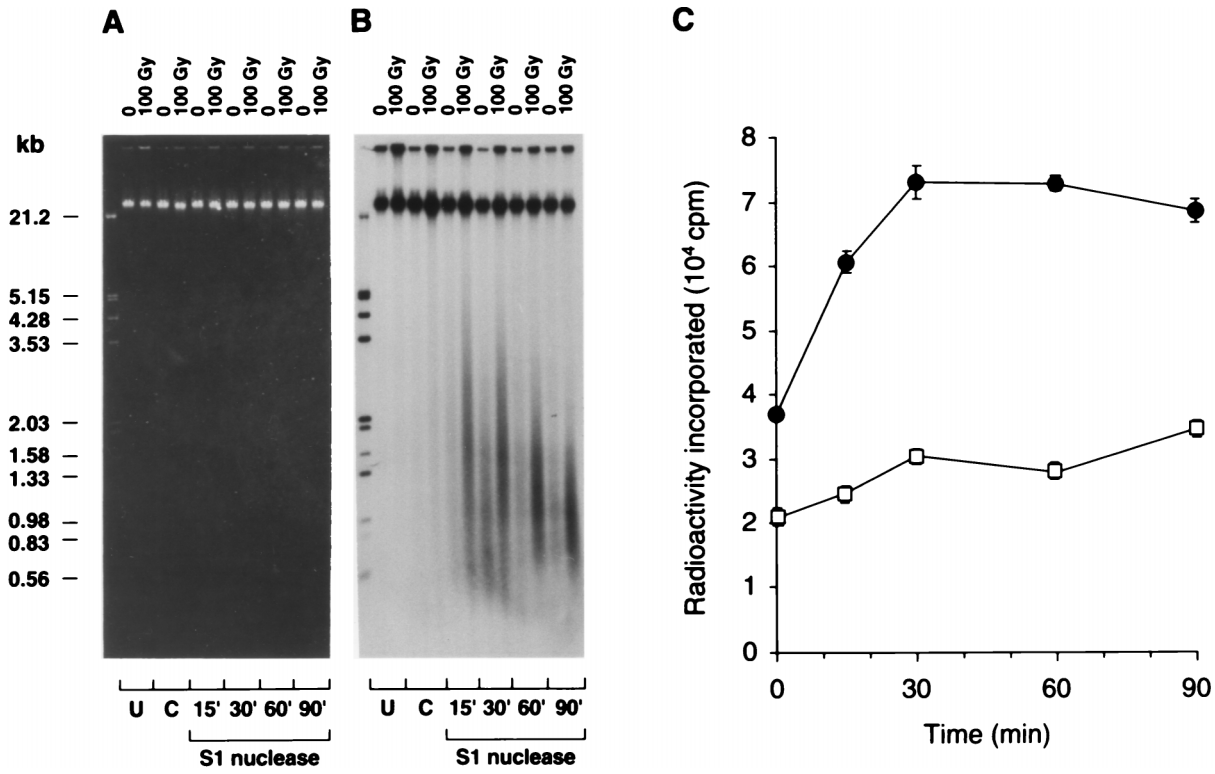

FIG. 7. Patterns of S1 nuclease cleavage obtained with DNA isolated from control and gamma-irradiated cells. T47D-Hygro-3 cells were gamma irradiated (100 Gy) on ice or untreated (control; lanes 0). DNA was isolated and incubated with S1 nuclease at 15°C (see Materials and Methods) for 15, 30, 60, and 90 min. All DNA samples (0.2 μg) were 3′ end labeled by T4 DNA polymerase with [α-^{32}P]dCTP. (A and B) Conventional agarose gels. U, DNA not treated with S1 nuclease or processed as S1 nuclease-treated samples; C, control incubation of DNA in the presence of S1 nuclease buffer but no S1 nuclease, with processing through phenol extraction as for S1 nuclease-treated samples. (A) Ethidium bromide staining pattern. (B) Autoradiogram (1 h at −70°C). (C) Radioactivity incorporated in gamma-irradiated (filled circles) or control (open squares) DNA after incubation with S1 nuclease for 0, 15, 30, 60, and 90 min, as measured by dot filtration. Data are means ± standard deviations for three determinations (triplicate DNA preparations).

naked DNA gamma irradiated in vitro. All DNA samples were treated with S1 nuclease and 3′ end labeled in the presence of endonuclease IV to remove 3′ blocking groups. The progressive radiation dose-dependent cleavage and disappearance of large DNA observed with the gamma-irradiated DNA, visible by both ethidium bromide staining (Fig. 8C) and autoradiography (Fig. 8D), is in sharp contrast with the discontinuous cleavage patterns observed following cell irradiation (Fig. 8A and B). Moreover, most cleavage of the gamma-irradiated DNA (Fig. 8C and D) resulted directly from irradiation and not from S1 nuclease-mediated cleavage (not shown). In contrast, little if any formation of fragments of <50 kb was detected in DNA from gamma-irradiated cells in the absence of S1 nuclease treatment (Fig. 7 and 8; see Fig. 10). This distinction further shows that both the nature and localization of DNA damage induced by ionizing radiation are radically different in naked DNA and chromatin of intact cells. While the cleavage patterns shown in Fig. 8C and D do correspond to those predicted for a quasi-random distribution of cleavage, the unique cleavage patterns shown in Fig. 7A and B, 8A and B, and 10 (see below) clearly suggest that chromatin structure was the primary determinant of the observed clustered distribution of S1 nuclease-detected DNA damage.

Use of endonuclease IV and S1 nuclease to monitor post-gamma irradiation DNA repair. Repair of AP sites and strand breaks containing phosphate or phosphoglycolate blocking groups at their 3′ ends, such as are produced by ionizing radiation and other sources of hydroxyl radicals, is thought to be initiated by cellular AP endonucleases. This initial repair can be assessed by 3′ end labeling in the presence or absence of endonuclease IV. Figure 9A shows an example of DNA repair kinetics measured in this way in human cells that were exposed to 100 Gy at 0°C and further incubated at 37°C under normal growth conditions. Following a small but significant increase of DNA damage detected during the first minute of postradiation incubation, DNA repair rates appeared to be biphasic, showing a fast component during the next 4 min followed by a much slower repair process. The decrease in 3′ end labeling measured in the presence of endonuclease IV reflects the simultaneous disappearance of strand breaks and AP sites. Only 3′-hydroxyl-containing strand interruptions are detected in the absence of endonuclease IV. If the decrease in label incorporation at 3′ ends (Fig. 9A) was due to ligation of single-strand breaks, one would expect a parallel progressive disappearance of single-strand breaks detected by S1 nuclease. This is precisely what was observed, as shown in Fig. 9B and C. Note that the kinetics of label disappearance in >50-kb and 0.5- to 2-kb S1 fragments (Fig. 9B), as well as in total unfractionated S1-treated DNA (Fig. 9C), are closely parallel to that of the disappearance of 3′-end label in the DNA that was not treated with S1 nuclease (Fig. 9A). However, in contrast to the biphasic kinetics observed for global loss of 3′ labeling and S1-hypersensitive sites (Fig. 9A and C), the disappearance of the small S1 fragments was monophasic, showing only the fast-kinetics component. Moreover, a progressive increase in DNA viscosity was also noticed (but not measured) during the postirradiation incubation of the cells. Together these observations therefore strongly suggest that the decrease in DNA

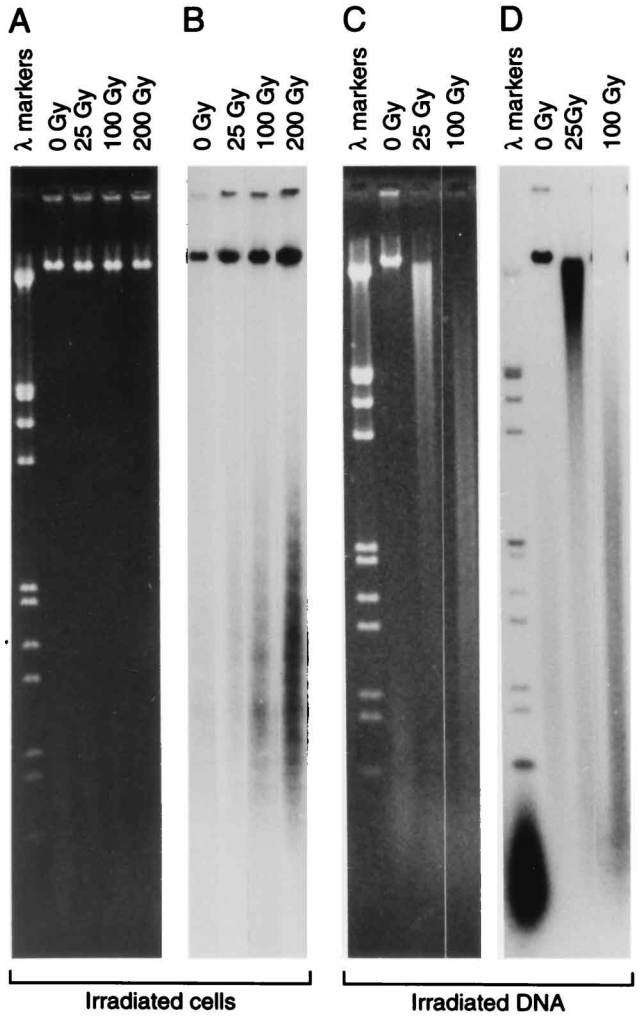

FIG. 8. Comparison of effects of gamma irradiation of cells versus naked DNA on DNA sensitivity to S1 nuclease-mediated cleavage. DNA isolated from T47D-Hygro-3 cells that were exposed to 0 (control), 25, 100, and 200 Gy on ice (A and B) and DNA from nonirradiated cells exposed to 0 (control), 25, and 100 Gy on ice (C and D) were incubated for 60 min with S1 nuclease at 15°C, and then 0.2 μg of each DNA sample was 3′ end labeled and analyzed by agarose gel electrophoresis as described in the legend to Fig. 7. (A and C) Ethidium bromide staining patterns; (B and D) autoradiograms.

end labeling and disappearance of S1 fragments were consequent to DNA repair and ligation. Note also that no repair of single-strand breaks was evident during 5 min of cell incubation at 0°C (Fig. 9B, last lane). The average half-life of single-strand breaks repaired at 37°C during the fast-kinetics component can be estimated to be about 2 to 3 min (Fig. 9B and C). Finally, the half-life of the lesions detected by endonuclease IV, including 3′ blocking groups plus AP sites, was estimated to be 1 to 2 min in several independent experiments with T47D-Hygro-3 cells.

Different types of DNA-damaging agents produce similar clustered distributions of S1 nuclease-hypersensitive sites in human cells and live mice. The pattern of S1 nuclease cleavage of DNA from gamma-irradiated cells (Fig. 7B, 8B, and 9B) could reflect preferential DNA damage in open chromatin regions containing locally exposed DNA. If so, such exposed DNA might be intrinsically hypersensitive to various types of DNA-damaging agents. In order to test this hypothesis, we have compared S1 cleavage patterns obtained with human cells exposed to ionizing radiation, menadione, MMS, or the topoisomerase II inhibitor streptonigrin. As shown in the left panel of Fig. 10, all agents yielded strikingly similar S1 nuclease cleavage patterns. Note the production and similar size distribution of S1 fragments in the range of 0.5 to 2 kb (visible in the bottom half of Fig. 10) obtained with all four DNA-damaging agents tested and that such fragments were not detected in the absence of S1 treatment. Note also the presence of trace amounts of such fragments detected in S1 nuclease-treated DNA of control cells, which were clearly visible in longer autoradiographic exposures (not shown). In order to verify that these cleavage patterns were not an artifact of the carcinoma cell line used in these experiments, we have compared them to S1 nuclease cleavage patterns obtained with DNAs of normal tissues from adult mice that were injected or not with MMS. The right panel of Fig. 10 shows S1 cleavage patterns obtained with DNAs extracted from kidneys and livers of MMS-treated mice as compared to cleavage obtained with DNA from menadione-treated cells (in the same gel). Duplicate lanes show the reproducibility of S1 hypersensitivity observed in two individual mice. As seen in Fig. 10, remarkably similar clustered distributions of MMS-induced S1 hypersensitive sites were observed in DNAs from cultured human cells and from normal mouse tissues.

DISCUSSION

The studies reported here display two original contributions. First, a novel procedure based on DNA 3′ end labeling in combination with an AP endonuclease was used to analyze quantitatively the average frequency of DNA strand breaks and AP sites in genomic DNA. Second, the combined use of S1 nuclease and DNA end labeling led to the discovery of an intriguing clustered distribution of DNA damage observed with various types of DNA-damaging agents to which mammalian cells were exposed.

Basal levels of DNA strand interruptions in mammalian cells. Both 3′ and 5′ end labeling data indicate an average DNA strand interruption frequency of about 0.15 to 0.3 per kb in proliferating cultured cells of human or mouse origin, and a similar frequency was found in several mouse tissues, such as liver and kidney of adult animals. In contrast, several other tissues, including skin and brain cortex, showed up to 10-fold more DNA end labeling, suggesting higher rates of DNA metabolism in these tissues. Several independent observations indicate that DNA replication contributed significantly to the basal levels of DNA strand interruptions in proliferating cells. These include a significant reduction of 3′ end labeling in DNA isolated from confluent cells or cells treated with DNA synthesis inhibitors and increased levels of 3′ termini in proliferating liver cells of newborn mice. The contribution of transient DNA cleavage catalyzed by topoisomerases and helicases, e.g., during transcription and chromosome condensation, is not known. It is of interest that some nonproliferative tissues, such as mouse brain cortex, showed exceptionally high levels of strand breaks and 3′-blocked termini or AP sites (endonuclease IV sensitive), suggesting intrinsically high levels of oxidative DNA damage in this tissue. These observations are in good agreement with the elevated levels of 8-oxodeoxyguanosine found in both nuclear and mitochondrial DNAs of human brain cortex (51). The origin of the small but significant increment of 3′ end labeling observed in the presence of endonuclease IV, in DNAs of both cultured cells and mouse tissues, is presently uncertain. This increment may at least

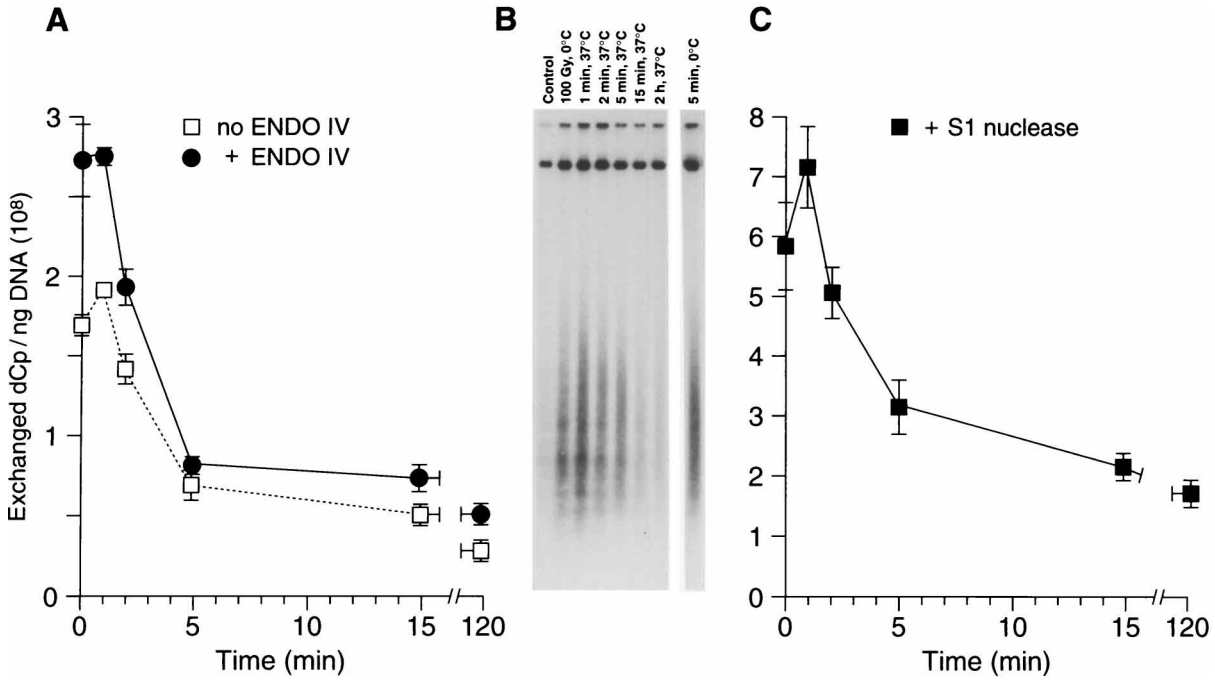

FIG. 9. Kinetics of DNA repair following gamma irradiation. Growing T47D-Hygro-3 cells were exposed to 100 Gy of gamma rays on ice and then incubated at 37°C for 1, 2, 5, 15, and 120 min and at 0°C for 5 min (in panel B). (A) Exchanged dCp at 3′ ends of cellular DNA treated or not with endonuclease IV, as measured by dot filtration. (B) Agarose gel autoradiogram of DNA incubated with S1 nuclease (60 min, 15°C) prior to 3′ end labeling. (C) Exchanged dCp at 3′ ends of cellular DNA incubated with S1 nuclease (same DNA samples as in panel B), as measured by dot filtration. Data are means ± standard deviations for three determinations (triplicate DNA preparations) from which the basal dCp exchange measured in DNA of unexposed cells was subtracted.

partly reflect the basal levels of AP sites and oxidative damage detected in cellular DNA of mammalian origin (47).

Quantification of DNA damage and repair in mammalian cells. The total frequency of strand breaks plus AP sites induced in gamma-irradiated T47D cells was estimated to be 4.6×10^{-3} lesion/kb/Gy, as calculated from linear regression between 0 and 200 Gy. This estimation turns out to be at least 1 order of magnitude larger than the frequency of alkali-sensitive lesions reported in previous studies with different cells, lower radiation dose exposures, and, above all, different techniques that were based on rates of DNA unwinding under alkaline conditions. One important factor thought to contribute massively to the larger frequency of DNA damage calculated from our 3′-end-labeling data is the novel detection of closely clustered strand breaks by the technique used in this study (discussed below). Indeed, most of these clustered breaks would have been overlooked by DNA-unwinding techniques. Our finding that 55 to 65% of the single-strand breaks could be 3′ end labeled by T4 DNA polymerase immediately after irradiation on ice, and thus contained 3′-hydroxyl groups, is in excellent agreement with early work of Lennartz et al. carried out with irradiated thymocytes (44). Such an important fraction of 3′-hydroxyl termini in irradiated cells stands in contrast with previous reports showing that DNA irradiated in vitro in phosphate buffer contained very few 3′-hydroxyl-containing termini accessible to DNA polymerases (29, 30). However, we found recently that DNA gamma irradiated in TE (10 mM Tris-HCl, 1 mM EDTA, pH 7.4) instead of phosphate buffer could be 3′ end labeled with T4 DNA polymerase (in the absence of endonuclease IV) to a similar extent as DNA isolated from gamma-irradiated cells (data not shown). These results strongly suggest that the nature of the immediate molecular environment around the DNA is a determining factor of the yield of 3′-hydroxyl-containing termini produced by ionizing radiation.

The DNA repair kinetics data we have presented illustrate the advantage of using the combination of 3′ end labeling, endonuclease IV, and S1 nuclease as probes to monitor repair of ionizing-radiation-induced DNA damage during postradiation incubation periods. We could show that processing of 3′ blocking groups plus AP sites and repair of single-strand breaks were both remarkably fast in human T47D cells, occurring within a few minutes during the initial phase of repair. The rapid disappearance of endonuclease IV-sensitive lesions observed after irradiation suggests that AP endonucleases and/or 3′-exonucleases are very active in these cells. Whether this is a specific feature of the cell line investigated or a common property of many human or mammalian cells remains to be determined. The rapid disappearance of bulk single-strand breaks observed in the T47D cells during the initial phase of postradiation repair is in good agreement with previous DNA repair studies carried out with rodent cell lines and human leukocytes and with different techniques (14, 77). It is of interest that the gamma ray-induced lesions giving rise to the small S1 nuclease fragments detected in this work belong to a class of very rapidly repaired single-strand breaks (see below).

Clustered distribution of in vivo-induced DNA damage detected by S1 nuclease. The most provocative finding of this study is the discovery of an apparently clustered distribution of DNA damage that was observed with several types of clastogenic agents. Analysis of both the frequency and distribution of DNA damage by use of the single-stranded-DNA-specific S1 nuclease has revealed unusual DNA cleavage patterns, characterized by the generation of short S1 fragments (0.5 to 2 kb) accounting for a very small fraction of total cellular DNA (<1%). Strikingly similar S1 cleavage patterns were obtained

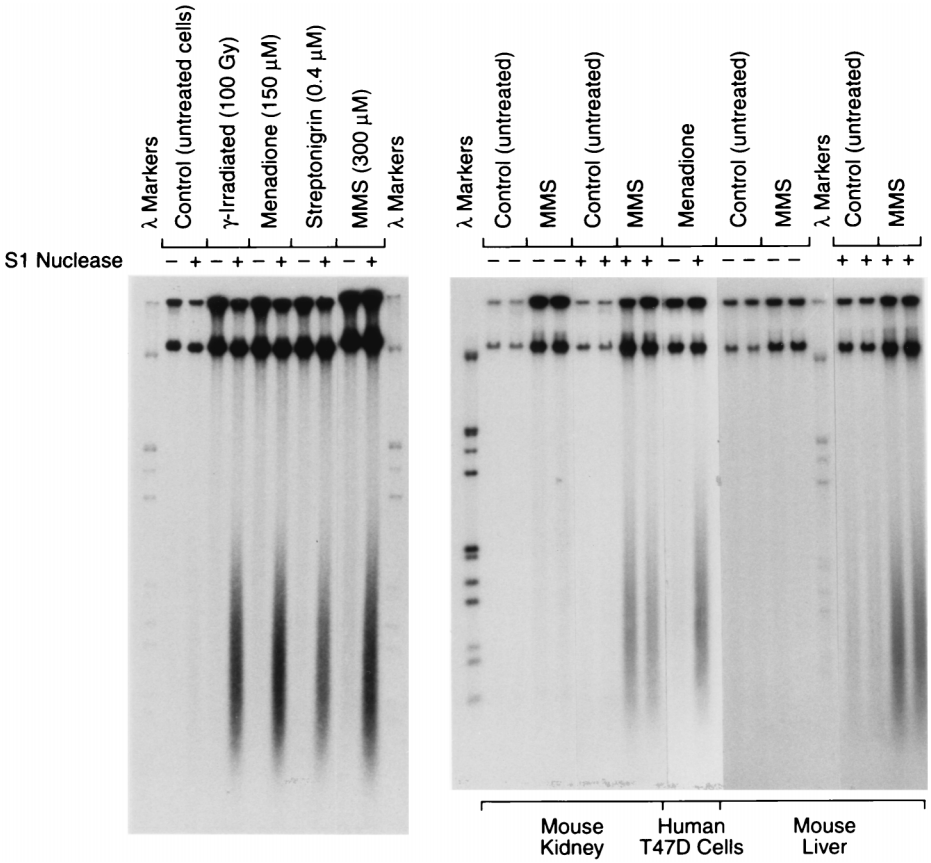

FIG. 10. Different types of DNA-damaging agents induce similar distribution patterns of S1 nuclease hypersensitivity. (Left panel) DNA of human T47D-Hygro-3 cells exposed to DNA-damaging agents as indicated. (Right panel) Liver and kidney DNAs of adult mice (duplicates) injected (i.p.) or not with MMS. S1 nuclease treatment, 3′ end labeling, and agarose gel electrophoresis were carried out as for Fig. 7.

with cultured cells exposed to ionizing radiation, menadione, singlet oxygen (data not shown), MMS, and topoisomerase II inhibitors, as well as with mice exposed to MMS in vivo. In contrast, a radically different cleavage pattern was obtained when isolated DNA was exposed to gamma irradiation and S1 digestion under strictly identical conditions. Two conclusions can be drawn from these observations: (i) the distribution of most S1 cleavage sites induced in living cells by the DNA-damaging agents tested was highly nonrandom, and (ii) the distribution of these S1-sensitive lesions was determined primarily by chromatin structure and not by DNA structure only. These findings raise a number of relevant questions.

First, what is the nature of these S1-sensitive lesions? Studies with plasmid DNA models (43) yielded the following answers: (i) double-stranded DNA, whether containing AP sites or not, was resistant to S1 nuclease treatment (under the stringent conditions used); (ii) DNA cleavage at DNA nicks was inefficient; and (iii) S1-resistant nicks could be converted to S1-sensitive sites by short exposure to 3′-exonucleolytic trimming to produce gaps. Therefore, the S1-hypersensitive sites induced in cellular DNA in response to the clastogenic agents used in this work are likely to consist primarily of single-strand interruptions such as sensitive nicks and gaps. The fact that 3′-exonucleolytic trimming prior to S1 nuclease cleavage of damaged DNA (MMS-treated cells) did not increase significantly the number of S1 fragments produced, i.e., did not reveal S1-resistant nicks, suggests that the S1 cleavage sites were essentially DNA gaps. The scarcity of MMS-induced S1-resistant nicks in the 0.5- to 2-kb S1 fragment fraction was confirmed independently by denaturation of the S1-treated DNA with glyoxal prior to gel electrophoresis. Moreover, in the absence of S1 nuclease treatment, glyoxal-mediated strand separation of this MMS-damaged DNA clearly revealed a range of fragments overlapping the size distribution of the S1 fragments described above (data not shown). This observation provides independent support for the presence of clustered DNA strand interruptions, without using S1 nuclease as a probe to detect them.

Are these S1-hypersensitive sites colocalized with initial DNA damage? This question is of obvious significance, since the induction of single-strand breaks could be a secondary event resulting from cellular responses to DNA damage. The most relevant responses include DNA repair, coupled or not to transcription (26), and potential induction of apoptosis. A conclusive answer to this question has not been obtained yet. In the case of our gamma radiation data, involvement of DNA repair and/or apoptotic processes could likely not account for the induction of S1-hypersensitive sites observed immediately after cell exposure to ionizing radiation in ice. In this case, the damage detected was probably restricted to "initial" induction of DNA strand breaks by radiation, with little if any contribution of strand breaks secondary to apoptosis or DNA repair responses. The rapid disappearance of most strand breaks during a few minutes of incubation after gamma irradiation clearly indicates that these strand breaks did not result from apoptotic DNA cleavage. The theoretical possibility of an immediate

DNA cleavage process occurring at 0°C as triggered by an initial DNA lesion cannot, however, be totally excluded.

Where are these S1-hypersensitive sites localized in the genome with respect to higher-order chromatin organization? Are the same chromatin regions preferentially sensitive to different types of DNA-damaging agents, and why should these DNA regions be preferentially sensitive to DNA damage? One attractive model that could explain localized preferential DNA damage, a putative colocalization of damage induced by different types of damaging agents, and the observed clustered distribution of DNA damage in the genome is based on the hypothetical existence of unpaired DNA in specific regions of the chromatin. Single-stranded DNA is known to be much more sensitive than double-stranded DNA to several types of DNA damage, including depurination and cytidine deamination (69); oxidants such as permanganate and osmium tetroxide are classic chemical probes used to detect unpaired DNA and Z-DNA structures. Junctions between B- and Z-DNA may also be sites hypersensitive to nucleases (70) and to DNA-damaging agents (63). On the other hand, there is indeed growing evidence for the existence of unpaired DNA in specific regions of chromatin (6, 35, 52, 61) and for the presence within the cell of S1-hypersensitive sites that were mapped close to SARs (MARs) (24, 74), previously defined as scaffold or matrix attachment regions (10, 39, 56). Single-stranded DNA was detected in SARs of the chicken α-globin gene domain (74) and in *cis* elements of the active human c-*myc* gene (52) and was implicated in the binding of lamina to SARs (50). On the other hand, there is accumulating evidence from the field of radiobiology that both the extent and distribution of DNA damage appear to depend on chromatin structure (for a review, see reference 65). Little is known, however, about the relative distribution of DNA damage and repair with regard to higher-order chromatin organization. It will thus be of interest to determine which regions of the chromatin are preferentially sensitive to DNA damage and cleavage. The knowledge that topoisomerase II binds preferentially to SARs (1) and is a structural component of mitotic chromosomes (17) suggests that the clusters of S1 cleavage sites induced by the topoisomerase II inhibitor streptonigrin (Fig. 10) were largely localized in SARs (or nuclear matrix), as this quinone is reported to target DNA cleavage via its binding to topoisomerase II, not to DNA (83). Whether the similar S1 cleavage patterns observed with the other DNA-damaging agents we have tested (e.g., gamma rays, MMS, and menadione) also reflect preferential DNA damage localization in SARs will have to be determined. It is of interest that repair of closely spaced single-strand breaks (giving rise to the family of small S1 fragments) induced by ionizing radiation was extremely fast. This may suggest that the DNA damage occurred at or close to sites where preformed multienzyme DNA repair complexes are localized on the nucleoskeleton or that the damaged DNA was rapidly recruited to such repair complexes. Recent data from the laboratory of P. Hanawalt have shown that recruitment of cyclobutane pyrimidine dimer-containing DNA to the nuclear matrix does occur during the initial phase of nucleotide excision repair following UV irradiation (36). This is consistent with the concept of DNA repair factories residing on the nuclear matrix (36).

The mechanism(s) by which mammalian cells sense DNA damage and mount adaptive responses, such as cell cycle arrest, DNA repair, and/or apoptosis, is far from being fully understood. One key factor identified in this process is the famous multifunctional p53 tumor suppressor protein, which is thought to act as the "guardian of the genome" (40). Among the multiple functions attributed to p53, nonspecific binding to short single-strand DNA stretches (34, 41) and the recently discovered 3′-to-5′ exonucleolytic activity (58) may be indicative of a dual role of p53 as potential sensor of DNA damage and partner of the DNA repair machinery. Interestingly, both wild-type and mutant p53 proteins have the property of binding to intact (undamaged) MAR/SAR elements, with the highest binding specificity associated with mutant p53 proteins (57). It would thus be of particular interest to determine in vitro to what extent DNA damage (e.g., single-strand breaks and gaps) may increase the binding affinity of wild-type p53 to SAR elements and to investigate in cells whether p53 colocalizes with preferential DNA damage in the nuclear matrix. Positive results may lead to the speculation that the coordinate presence of damage-hypersensitive DNA elements and p53 in the nuclear matrix may be part of one mechanism permitting sensing of DNA damage and triggering of appropriate p53-mediated cellular responses according to DNA damage severity. Besides, the putative presence of hypersensitive DNA elements in the nuclear matrix could contribute to an increase in the frequency of illegitimate recombination and translocations that can involve breakpoints within MAR elements (71).

Preliminary experiments carried out in vitro with plasmid DNAs have shown that a SAR-containing DNA segment from a *Drosophila melanogaster hsp70* gene locus (56) was intrinsically hypersensitive to acid-catalyzed depurination or bleomycin-mediated DNA cleavage in supercoiled plasmids and displayed strikingly similar fine-structure localization of DNA damage (43). Whether this preferential localization of DNA damage reflects a localized DNA-unpairing tendency and is SAR specific is currently under investigation. The real challenge to test our model will be to find the best way to investigate the putative relationships between the distribution of preferential DNA damage, localized DNA single strandedness, and higher-order chromatin structure in living cells.

ACKNOWLEDGMENTS

This work was supported by the National Cancer Institute of Canada with funds provided by the Canadian Cancer Society (grants 3488 and 4543 to M.-E.M.). D.R. is a scholar of the National Cancer Institute of Canada. J.L. was the recipient of studentships from the Natural Sciences and Engineering Research Council of Canada and from the FCAR.

We thank Guy Poirier and Regen Drouin for critical reading of the manuscript and helpful discussions.

REFERENCES

1. **Adachi, Y., E. Käs, and U. K. Laemmli.** 1989. Preferential, cooperative binding of DNA topoisomerase II to scaffold-associated regions. EMBO J. **8:**3997–4006.
2. **Ames, B. N.** 1989. Endogenous DNA damage as related to cancer and aging. Mutat. Res. **214:**41–46.
3. **Ames, B. N., M. K. Shigenaga, and T. M. Hagen.** 1993. Oxidants, antioxidants, and the degenerative diseases of aging. Proc. Natl. Acad. Sci. USA **90:**7915–7922.
4. **Aruoma, O. I., B. Halliwell, and M. Dizdaroglu.** 1989. Iron ion-dependent modification of bases in DNA by the superoxide radical-generating system hypoxanthine/xanthine oxidase. J. Biol. Chem. **264:**13024–13028.
5. **Birnboim, H. C., and J. J. Jevcak.** 1981. Fluorometric method for rapid detection of DNA strand breaks in human white blood cells produced by low doses of radiation. Cancer Res. **41:**1889–1892.
6. **Bode, J., Y. Kohwi, L. Dickinson, T. Joh, D. Klehr, C. Mielke, and T. Kohwi-Shigematsu.** 1992. Biological significance of unwinding capability of nuclear matrix-associating DNAs. Science **225:**195–197.
7. **Challberg, M. D., and P. T. Englund.** 1980. Specific labeling of 3′ termini with T4 DNA polymerase. Methods Enzymol. **65:**39–42.
8. **Chen, G. L., Y. Yang, T. C. Rowe, B. D. Galligan, K. M. Tewey, and L. F. Liu.** 1984. Nonintercalative antitumor drugs interfere with the breakage-reunion reaction of mammalian DNA topoisomerase II. J. Biol. Chem. **259:**13560–13566.
9. **Ciccarone, V., B. A. Spengler, M. B. Meyers, J. L. Biedler, and R. A. Ross.** 1989. Phenotypic diversification in human neuroblastoma cells: expression of

distinct neural crest lineages. Cancer Res. **49:**219–225.
10. **Cockerill, P. N., and W. T. Garrard.** 1986. Chromosomal loop anchorage of the kappa immunoglobulin gene occurs next to the enhancer in a region containing topoisomerase II sites. Cell **44:**273–282.
11. **Cohen, M. S., Y. Chai, B. E. Britigan, W. McKenna, J. Adams, T. Svendsen, K. Bean, D. J. Hassett, and P. F. Sparling.** 1987. Role of extracellular iron in the action of the quinone antibiotic streptonigrin: mechanisms of killing and resistance of *Neisseria gonorrhoeae*. Antimicrob. Agents Chemother. **31:**1507–1513.
12. **Coquerelle, T., A. Bopp, B. Kessler, and U. Hagen.** 1973. Strand breaks and 5′ end-groups of irradiated thymocytes. Int. J. Radiat. Biol. **24:**397–404.
13. **Demple, B., and L. Harrison.** 1994. Repair of oxidative damage to DNA: enzymology and biology. Annu. Rev. Biochem. **63:**915–948.
14. **Dikomey, E., M. Flentje, and J. Dahm Daphi.** 1995. Comparison between the alkaline unwinding technique and neutral filter elution using CHO, V79 and EAT cells. Int. J. Radiat. Biol. **67:**269–275.
15. **Dizdaroglu, M.** 1994. Chemical determination of oxidative DNA damage by gas chromatography-mass spectroscopy. Methods Enzymol. **234:**3–16.
16. **Dworniczak, B., and M.-E. Mirault.** 1987. Structure and expression of a human gene coding for a 71 Kd heat shock "cognate" protein. Nucleic Acids Res. **15:**5181–5197.
17. **Earnshaw, W. C., B. Halligan, C. A. Cooke, M. M. S. Heck, and L. F. Liu.** 1985. Topoisomerase II is a structural component of mitotic chromosome scaffolds. J. Cell Biol. **100:**1706–1715.
18. **Egan, M. P., and D. Herrick.** 1982. The effect of ara-C incorporation on DNA synthesis. Biochem. Pharmacol. **31:**2937–2940.
19. **Fridovich, I.** 1986. Biological effects of the superoxide radical. Arch. Biochem. Biophys. **247:**1–11.
20. **Friedberg, E. C.** 1985. DNA repair. W. H. Freeman & Co., New York, N.Y.
21. **Gao, S., R. Drouin, and G. P. Holmquist.** 1994. DNA repair rates mapped along the human PGK1 gene at nucleotide resolution. Science **263:**1438–1440.
22. **Gavrieli, Y., Y. Sherman, and S. A. Ben Sasson.** 1992. Identification of programmed cell death in situ via specific labeling of nuclear DNA fragmentation. J. Cell Biol. **119:**493–501.
23. **Gorczyca, W., J. Gong, and Z. Darzynkiewicz.** 1993. Detection of DNA strand breaks in individual apoptotic cells by the in situ terminal deoxynucleotidyl transferase and nick translation assays. Cancer Res. **53:**1945–1951.
24. **Gromova, I. I., O. F. Nielsen, and S. V. Razin.** 1995. Long-range fragmentation of the eukaryotic genome by exogenous and endogenous nucleases proceeds in a specific fashion via preferential DNA cleavage at matrix attachment sites. J. Biol. Chem. **270:**18685–18690.
25. **Halliwell, B., and O. I. Aruoma.** 1991. DNA damage by oxygen-derived species: its mechanism and measurement in mammalian systems. FEBS Lett. **281:**9–19.
26. **Hanawalt, P. C., B. A. Donahue, and K. S. Sweder.** 1994. Repair and transcription. Collision or collusion? Curr. Biol. **4:**518–521.
27. **Haring, M., H. Rudiger, B. Demple, S. Boiteux, and B. Epe.** 1994. Recognition of oxidized abasic sites by repair endonucleases. Nucleic Acids Res. **22:**2010–2015.
28. **Hassett, D., B. E. Britigan, T. Svendsen, G. M. Rosen, and M. S. Cohen.** 1987. Bacteria form intracellular free radicals in response to paraquat and streptonigrin: demonstration of the potency of hydroxyl radical. J. Biol. Chem. **262:**13404–13408.
29. **Henner, W. D., S. M. Grunberg, and W. A. Haseltine.** 1983. Enzyme action at 3′ termini of ionizing radiation-induced DNA strand breaks. J. Biol. Chem. **258:**15198–15205.
30. **Henner, W. D., L. O. Rodriguez, S. M. Hecht, and W. Haseltine.** 1983. Gamma-ray induced deoxyribonucleic acid strand breaks. J. Biol. Chem. **258:**711–713.
31. **Holmquist, G. P.** 1994. Chromatin self-organization by mutation bias. J. Mol. Evol. **39:**436–438.
32. **Ide, H., K. Akamatsu, Y. Kimura, K. Michiue, K. Makino, A. Asaeda, Y. Takamori, and K. Kubo.** 1993. Synthesis and damage specificity of a novel probe for the detection of abasic sites in DNA. Biochemistry **32:**8276–8283.
33. **Imlay, J. A., and S. Linn.** 1988. DNA damage and oxygen radical toxicity. Science **240:**1302–1309.
34. **Jayaraman, J., and C. Prives.** 1995. Activation of p53 sequence-specific DNA binding by short single strands of DNA requires the p53 C-terminus. Cell **81:**1021–1029.
35. **Kay, V., and J. Bode.** 1994. Binding specificity of a nuclear scaffold: supercoiled, single-stranded, and scaffold-attached-region DNA. Biochemistry **33:**367–374.
36. **Koehler, D. R., and P. C. Hanawalt.** 1996. Recruitment of damaged DNA to the nuclear matrix in hamster cells following ultraviolet irradiation. Nucleic Acids Res. **24:**2877–2884.
37. **Kohn, K. W., L. C. Erickson, R. A. G. Ewig, and C. A. Friedman.** 1976. Fractionation of DNA from mammalian cells by alkaline elution. Biochemistry **15:**4629–4637.
38. **Kubo, K., H. Ide, S. S. Wallace, and Y. W. Kow.** 1992. A novel, sensitive, and specific assay for abasic sites, the most commonly produced DNA lesion. Biochemistry **31:**3703–3708.
39. **Laemmli, U. K., E. Käs, L. Poljak, and Y. Adachi.** 1992. Scaffold-associated regions: cis-acting determinants of chromatin structural loops and functional domains. Curr. Opin. Genet. Dev. **2:**275–285.
40. **Lane, D. P.** 1992. p53, guardian of the genome. Nature **358:**15–16.
41. **Lee, S., B. Elenbaas, A. Levine, and J. Griffith.** 1995. p53 and its 14 kDa C-terminal domain recognize primary DNA damage in the form of insertion/deletion mismatches. Cell **81:**1013–1020.
42. **Legault, J.** 1995. M.Sc. thesis. Laval University, Quebec City, Canada.
43. **Legault, J., A. Tremblay, and M.-E. Mirault.** Preferential localization of DNA damage induced by depurination and bleomycin in a plasmid containing a scaffold-associated region. Biochem. Cell Biol., in press.
44. **Lennartz, M., T. Coquerelle, A. Bopp, and U. Hagen.** 1975. Oxygen—effect on strand breaks and specific end-groups in DNA of irradiated thymocytes. Int. J. Radiat. Biol. **27:**577–587.
45. **Levin, J. D., and B. Demple.** 1990. Analysis of class II (hydrolytic) and class I (β-lyase) apurinic/apyrimidinic endonucleases with a synthetic DNA substrate. Nucleic Acids Res. **18:**5069–5075.
46. **Levin, J. D., A. W. Johnson, and B. Demple.** 1988. Homogeneous Escherichia coli endonuclease IV: characterization of an enzyme that recognizes oxidative damage in DNA. J. Biol. Chem. **263:**8066–8071.
47. **Lindahl, T.** 1993. Instability and decay of the primary structure of DNA. Nature **362:**709–715.
48. **Liu, L. F.** 1989. DNA topoisomerase poisons as antitumor drugs. Annu. Rev. Biochem. **58:**351–375.
49. **Ljungman, M., and P. C. Hanawalt.** 1992. Efficient protection against oxidative DNA damage in chromatin. Mol. Carcinog. **5:**264–269.
50. **Luderus, M. E., J. L. den Blaauwen, O. J. de Smit, D. A. Compton, and R. van Driel.** 1994. Binding of matrix attachment regions to lamin polymers involves single-stranded regions and the minor groove. Mol. Cell. Biol. **14:**6297–6305.
51. **Mecocci, P., U. MacGarvey, A. E. Kaufman, D. Koontz, J. M. Shoffner, D. C. Wallace, and M. F. Beal.** 1993. Oxidative damage to mitochondrial DNA shows marked age-dependent increases in human brain. Ann. Neurol. **34:**609–616.
52. **Michelotti, G. A., E. F. Michelotti, A. Pullner, R. C. Duncan, D. Eick, and D. Levens.** 1996. Multiple single-stranded *cis* elements are associated with active chromatin of the human c-*myc* gene in vivo. Mol. Cell. Biol. **16:**2656–2669.
53. **Miller, S. A., D. D. Dykes, and H. F. Polesky.** 1988. A simple salting out procedure for extracting DNA from human nucleated cells. Nucleic Acids Res. **16:**1215.
54. **Mirault, M.-E., A. Tremblay, N. Beaudouin, and M. Tremblay.** 1991. Overexpression of seleno-glutathione peroxidase by gene transfer enhances the resistance of T47D human breast cells to clastogenic oxidants. J. Biol. Chem. **266:**20752–20760.
55. **Mirault, M.-E., A. Tremblay, L. Lavoie, M. Tremblay, and N. Beaudoin.** 1992. Transgenic expression of glutathione peroxidase in human breast cells: increased resistance to clastogenic oxidants, p. 303–306. *In* A. J. Jesaitis and E. A. E. Dratz (ed.), The molecular basis of oxidative damage by leukocytes. CRC Press, Boca Raton, Fla.
56. **Mirkovitch, J., M.-E. Mirault, and U. K. Laemmli.** 1984. Organization of the higher-order chromatin loop: specific DNA attachment sites on nuclear scaffold. Cell **39:**223–232.
57. **Muller, B. F., D. Paulsen, and W. Deppert.** 1996. Specific binding of MAR/SAR DNA-elements by mutant p53. Oncogene **12:**1941–1952.
58. **Mummenbrauer, T., F. Janus, B. Muller, L. Wiesmuller, W. Deppert, and F. Grosse.** 1996. p53 protein exhibits 3′-to-5′ exonuclease activity. Cell **85:**1089–1099.
59. **Pfeifer, G. P., R. Drouin, A. D. Riggs, and G. P. Holmquist.** 1992. Binding of transcription factors creates hot spots for UV photoproducts in vivo. Mol. Cell. Biol. **12:**1798–1804.
60. **Pfeifer, G. P., R. Drouin, A. D. Riggs, and G. P. Holmquist.** 1991. In vivo mapping of a DNA adduct at nucleotide resolution: detection of pyrimidine (6-4) pyrimidone photoproducts by ligation-mediated polymerase chain reaction. Proc. Natl. Acad. Sci. USA **88:**1374–1378.
61. **Pfeifer, G. P., and A. D. Riggs.** 1991. Chromatin differences between active and inactive X chromosomes revealed by genomic footprinting of permeabilized cells using DNase I and ligation-mediated PCR. Genes Dev. **5:**1102–1113.
62. **Ramotar, D., and B. Demple.** 1993. Enzymes that repair oxidative damage to DNA, p. 165–191. *In* B. H. O. I. Aruoma (ed.), DNA and free radical. Ellis Horwood, West Sussex, United Kingdom.
63. **Rodolfo, C., A. Lanza, S. Tornaletti, G. Fronza, and A. M. Pedrini.** 1994. The ultimate carcinogen of 4-nitroquinoline 1-oxide does not react with Z-DNA and hyperreacts with B-Z junctions. Nucleic Acids Res. **22:**314–320.
64. **Rodriguez, H., R. Drouin, G. P. Holmquist, T. R. O'Connor, S. Boiteux, J. Laval, J. H. Doroshow, and S. A. Akman.** 1995. Mapping of copper/hydrogen peroxide-induced DNA damage at nucleotide resolution in human genomic DNA by ligation-mediated polymerase chain reaction. J. Biol. Chem. **270:**17633–17640.
65. **Roti Roti, J. L., W. D. Wright, and Y. C. Taylor.** 1993. DNA loop structure and radiation response. Adv. Radiat. Biol. **17:**227–259.

66. **Roychoudhury, R., and R. Wu.** 1980. Terminal transferase-catalyzed addition of nucleotides to the 3′ termini of DNA. Methods Enzymol. **65:**43–51.
67. **Rydberg, B.** 1980. Detection of induced DNA strand breaks with improved sensitivity in human cells. Radiat. Res. **81:**492–495.
68. **Sambrook, J., E. F. Fritsch, and T. Maniatis.** 1989. Molecular cloning: a laboratory manual, 2nd ed. Cold Spring Harbor Laboratory, Cold Spring Harbor, N.Y.
69. **Shapiro, R.** 1981. Damage to DNA caused by hydrolysis. Plenum Publishing Corp., New York, N.Y.
70. **Singleton, C. K., J. Klysik, S. M. Stirdivant, and R. D. Wells.** 1982. Left-handed Z-DNA is induced by supercoiling in physiological ionic conditions. Nature **299:**312–316.
71. **Sperry, A. O., V. C. Blasquez, and W. T. Garrard.** 1989. Dysfunction of chromosomal loop attachment sites: illegitimate recombination linked to matrix association regions and topoisomerase II. Proc. Natl. Acad. Sci. USA **86:**5497–5501.
72. **Spivak, G., and P. C. Hanawalt.** 1996. Fine structure mapping of DNA repair within a 100 kb genomic region in Chinese hamster ovary cells. Mutat. Res. **350:**207–216.
73. **Stamato, T., and N. Denko.** 1990. Asymmetric field inversion gel electrophoresis: a new method for detecting DNA double-strand breaks in mammalian cells. Radiat. Res. **121:**196–205.
74. **Targa, F. R., S. V. Razin, C. V. de Moura Gallo, and K. Scherrer.** 1994. Excision close to matrix attachment regions of the entire chicken alpha-globin gene domain by nuclease S1 and characterization of the framing structures. Proc. Natl. Acad. Sci. USA **91:**4422–4426.
75. **Thor, H., M. T. Smith, P. Hartzell, G. Bellomo, S. A. Jewell, and S. Orrenius.** 1982. The metabolism of menadione (2-methyl-1,4-naphthoquinone) by isolated hepatocytes: a study of the implications of oxidative stress in intact cells. J. Biol. Chem. **257:**12419–12425.
76. **Tilly, J. L., K. I. Kowalski, A. L. Johnson, and A. J. Hsueh.** 1991. Involvement of apoptosis in ovarian follicular atresia and postovulatory regression. Endocrinology **129:**2799–2801.
77. **Van der Schans, G. P., A. A. W. M. Van Loon, R. H. Groenendijk, and R. A. Baan.** 1989. Detection of DNA damage in cells exposed to ionizing radiation by use of anti-single-stranded DNA monoclonal antibody. Int. J. Radiat. Biol. **55:**747–760.
78. **von Sonntag, C.** 1987. The chemical basis of radiation biology, p. 116–166, 221–294. Taylor and Francis, London, United Kingdom.
79. **Wallace, S. S.** 1988. AP endonucleases and DNA glycosylases that recognize oxidative DNA damage. Environ. Mol. Mutagen. **12:**431–477.
80. **Weinfeld, M., and G. W. Buchko.** 1993. Postlabelling methods for the detection of apurinic sites and radiation-induced DNA damage. IARC Sci. Publ. **124:**95–103.
81. **Weinfeld, M., M. Liuzzi, and M. C. Paterson.** 1990. Response of phage T4 polynucleotide kinase toward dinucleotides containing apurinic sites: design of a ^{32}P-postlabeling assay for apurinic sites in DNA. Biochemistry **29:**1737–1743.
82. **Weinfeld, M., and K. J. Soderlind.** 1991. ^{32}P-postlabeling detection of radiation-induced DNA damage: identification and estimation of thymine glycols and phosphoglycolate termini. Biochemistry **30:**1091–1097.
83. **Yamashita, Y., S. Kawada, N. Fujii, and H. Nakano.** 1990. Induction of mammalian DNA topoisomerase II dependent DNA cleavage by antitumor antibiotic streptonigrin. Cancer Res. **50:**5841–5844.